

# LEVEL

42

AD A 074595

REPORT MCR 79-632

## PROPULSION OPTIONS FOR THE HI SPOT LONG ENDURANCE DRONE AIRSHIP

W.L. Marcy  
R.O. Hookway  
MARTIN MARIETTA CORPORATION  
P.O. Box 179  
Denver, Colorado 80201

DDC  
RECEIVED  
OCT 3 1979  
E

15 SEPTEMBER 1979

### FINAL REPORT

DDC FILE COPY

PREPARED FOR:

NAVAL AIR DEVELOPMENT CENTER  
Code 6096  
Warminster, Pa 18974

This document has been approved  
for public release and sale; its  
distribution is unlimited.

79 10 01 023

## **DISCLAIMER NOTICE**

**THIS DOCUMENT IS BEST QUALITY PRACTICABLE. THE COPY FURNISHED TO DTIC CONTAINED A SIGNIFICANT NUMBER OF PAGES WHICH DO NOT REPRODUCE LEGIBLY.**

UNCLASSIFIED

SECURITY CLASSIFICATION OF THIS PAGE (When Data Entered)

REPORT DOCUMENTATION PAGE		READ INSTRUCTIONS BEFORE COMPLETING FORM
1. REPORT NUMBER NADC 78193-60	2. GOVT ACCESSION NO.	3. RECIPIENT'S CATALOG NUMBER
4. TITLE (and Subtitle) Propulsion Options for the HI SPOT Long Endurance Drone Airship		5. TYPE OF REPORT & PERIOD COVERED Final Report Nov 1978 - Sep 1979
7. AUTHOR(s) William L. Marcy Ralph O. Hookway		6. PERFORMING ORG. REPORT NUMBER MCR 79-632
9. PERFORMING ORGANIZATION NAME AND ADDRESS Martin Marietta Corporation, Denver Division P.O. Box 179 Denver, Colorado 80201		8. CONTRACT OR GRANT NUMBER(s) N62269-79-C-0204
11. CONTROLLING OFFICE NAME AND ADDRESS Naval Air Development Center Code 6096 Warminster, Pennsylvania, 18974		10. PROGRAM ELEMENT, PROJECT, TASK AREA & WORK UNIT NUMBERS
14. MONITORING AGENCY NAME & ADDRESS (if different from Controlling Office)		12. REPORT DATE 15 September 1979
		13. NUMBER OF PAGES 57
		15. SECURITY CLASS. (of this report) UNCLASSIFIED
		15a. DECLASSIFICATION/DOWNGRADING SCHEDULE
16. DISTRIBUTION STATEMENT (of this Report)  Approved for Public Release; Distribution Unlimited		
17. DISTRIBUTION STATEMENT (of the abstract entered in Block 20, if different from Report)		
19. SUPPLEMENTARY NOTES		
20. KEY WORDS (Continue on reverse side if necessary and identify by block number) Aerostats, Airships, Remotely Piloted Vehicles, Inflatable Structures, Airbreathing Propulsion		
21. ABSTRACT (Continue on reverse side if necessary and identify by block number) Airbreathing, monofueled, stored-energy, and solar-rechargeable propulsion systems have been studied for the HI SPOT Long Endurance Drone Airship, providing constant-level electrical power as well as variable aerodynamic thrust to maintain position in winds varying from 15 to 100 knots at high altitude. A hydrogen fueled airbreathing engine is optimum for mission lengths up to 30 days or more.		

DD FORM 1 JAN 73 1473

EDITION OF 1 NOV 65 IS OBSOLETE

UNCLASSIFIED  
SECURITY CLASSIFICATION OF THIS PAGE (When Data Entered)

# FOREWORD

This report is Item A002, Final Technical Report, of the Contract Data Requirements List to Contract N 62269-79-C-0204 between the Naval Air Development Center, Warminster, PA, and the Martin Marietta Aerospace, Denver Division, Denver, CO. This contract was performed from November 1978 to August 1979 at Denver, Colorado. The NADC Program Monitor was Mr. John A. Eney of the Lighter-Than-Air Systems Technology Office; the Program Manager for Martin Marietta Aerospace was Mr. William L. Marcy. This Final Report completes the data requirements of the contract.

Accession For	
MTIS GEMAI	<input checked="" type="checkbox"/>
DOC TAB	<input type="checkbox"/>
Unannounced	<input type="checkbox"/>
Justification	
By _____	
Distribution/	
Availability Codes	
Dist	Avail and/or special
A	

## Introduction

From 1974 to 1976, the U.S. Navy sponsored a high altitude, powered, unmanned, super pressure aerostat designed to keep station (within 50 nautical miles) in winds from 15 to 25 knots at approximately 68,000 feet altitude. This program, called HASPA, resulted in a conventional airship hull shape displacing 800,000 cubic feet and possessing 3,590 pounds of useful lift. A stern-mounted electric motor and gear reduction system drove a 26-foot propeller at 144 rpm, producing an estimated 37 pounds of thrust at altitude with 80% efficiency. In the operational concept, the vehicle was to be powered by an array of solar cells for daytime operation and a regenerative fuel cell for night operation (the fuel cell would be recharged by additional solar arrays during daylight). Four test vehicles were built, but due to minor malfunctions of procedure and of hardware, the first two vehicles launched were unsuccessful. As a result, the program was halted and directed to perform research on components, rather than complete airships, until a high probability of operational success could be assured.

One notable aspect of the vehicle was that, of the 3,590 pounds of vehicle weight, the propulsion system was allotted 1,540 pounds to produce 3.13 net horsepower at maximum speed, and an average of only 0.93 net HP. Inasmuch as gasoline engines are available weighing only a few pounds, and allowing a factor of 20 for the low air density at high altitude, it appears that a suitable powerplant could be had for as little as 100 pounds; allowing 200 pounds for a propeller and reduction drive still leaves more than 1,200 pounds for a fuel system, and this would be sufficient for more than 2,000 hours at cruise speeds. In 1978 the Navy awarded Martin Marietta Aerospace a contract to study alternative propulsion systems for the high altitude aerostat, now named HI SPOT (High Altitude Surveillance Platform for Over-the-Horizon Targeting). The results of that study are the subject of this report. Appendix "A" presents a summary of control studies performed to define autopilot requirements; Appendix "B" presents the equations derived for determining aerostat sizes and weights; and Appendix "C" summarizes technical contacts and document references used in the study.

The study addressed two tasks: first, a survey of current propulsion technology applicable to high altitude aerostats; and second, the application of current technology to aerostats performing a specific mission. At the same time, the Navy itself addressed the problems of payloads, duration at altitude, and upper-altitude winds, resulting in modification of the original HASPA operational requirements. For the purposes of the study, the following requirements were set by the Navy:

Payload - 200 lb., requiring 800 watts continuous electrical power

Duration = 30 days minimum

Wind Penetration Capability = 40 to 100 kt

Average Speed = 15 to 47 kt

Station Keeping within 50 nautical miles

Altitude = 100 to 50 millibars - Altitude keeping not required

#### Propulsion System Requirements

One of the most heavily criticized aspects of the HASPA program was that its maximum speed of 25 knots was inadequate for station keeping much of the time. While it is true that the Northern hemisphere annual average wind at the 50 millibar pressure level is about 15 knots, with a standard deviation of less than 10 knots, it is also true that there are months in which the average wind exceeds 40 knots, with 3 $\sigma$  peaks of 110 knots or more. An aerostat must therefore have a speed capability approaching 100 knots if it is to have a high probability of station keeping at any given place and time, even though its average speed over a long period may be only 15 knots or less. Power required increases approximately as the cube of air-speed; as shown in Figure 1, the 800,000 ft.<sup>3</sup> HASPA which requires only 2.8 thrust HP at 25 knots requires 139 HP at 100 knots; a proportional increase in the propulsion system weight would result in a value of 34.2 tons. Clearly, it is virtually impossible to brute-force this problem, and other means must be sought.

HASPA operated in a length Reynolds number range from 4.3 to 7.2 million; at 100 knots, its Reynolds number would be just under 30 million. In this range, the turbulent-flow drag coefficient (on  $V^{2/3}$ ) varies from .025 to .022. In 1966, B. H. Carmichael (AIAA paper 66-657, Ref. 1) reported on some experiments with shaped bodies in which he measured a drag coefficient of .0065 at

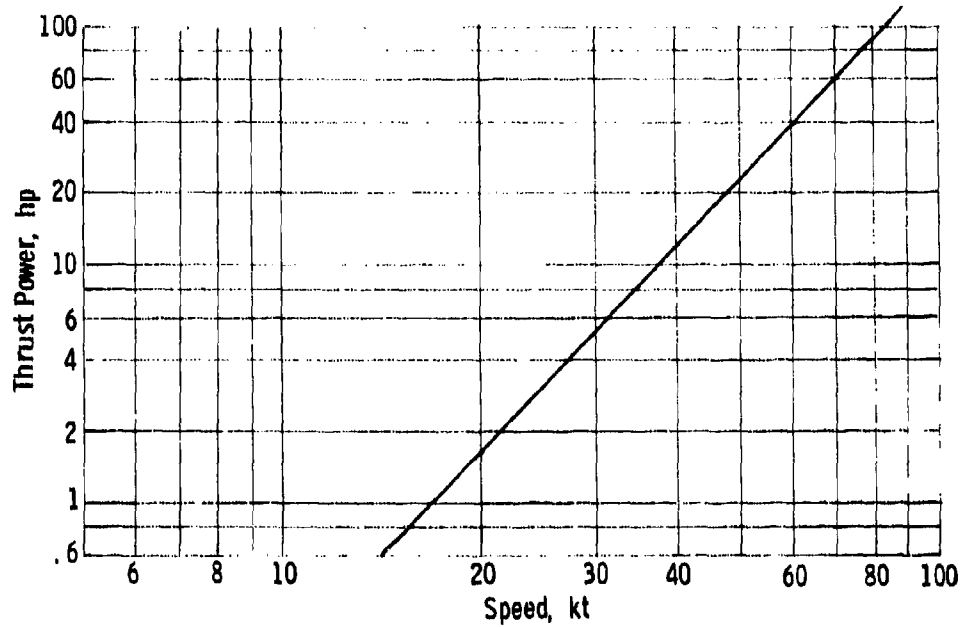


Figure 1: HASPA Power Required at Higher Speed

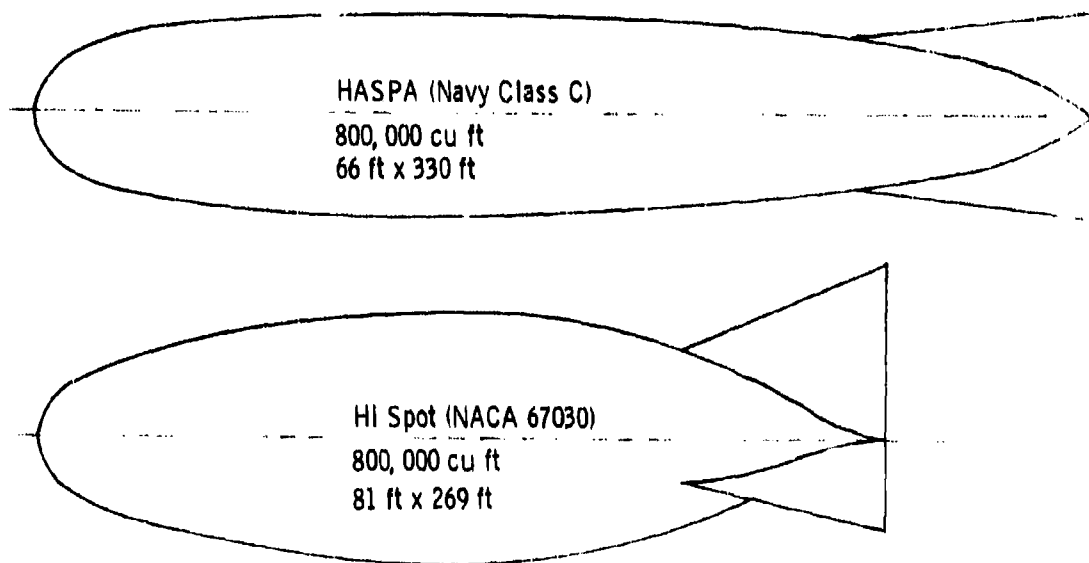


Figure 2: Comparison of Hull Profiles

23 million Reynolds number. Figure 2 compares Carmichael's hull shape with the HASPA hull, and Figure 3 compares his drag data with the HASPA estimates and with theoretical turbulent and laminar drag coefficients. The laminar type, low drag flow obtained by Carmichael is assured, despite the roughness of a hull made up of a grid of Kevlar yarn laid over a mylar film, by the low Reynolds number of the high altitude environment. As presented in Reference 2, the Reynolds number required of a transverse wire to trip a laminar boundary layer is about 900, based on the wire diameter. A HI SPOT aerostat flying at 50 kt airspeed at 65,000 feet has a Reynold's number of about 4,000 per inch, resulting in transverse strand Reynolds numbers of about 80; this is an order of magnitude less than that required to induce transition.

At 100 knots, an 800,000 ft.<sup>3</sup> aerostat with Carmichael's hull would require only 51.3 thrust HP. While this might require as much as 25,000 lb. of solar cells, fuel cells, electric motors, and so on, based on the HASPA system weights, the rotating machinery itself could weigh as little as 500 lb., and remembering that average power required at 15 knots would be less than 1/5 HP ( $51.3 \times .15^3$ ), a fueled propulsion system might operate for 30 days with as little as 150 lb. of fuel. We therefore use the hull form developed by Carmichael for the HI SPOT system, with a 25% increase in drag assumed as an allowance for fin, gondola, suspension, and interference drag; correspondingly, we consider powerplants in the 5 to 50 HP range, powering aerostats from 100,000 to 1,000,000 ft.<sup>3</sup> at speeds from 15 to 100 kt for our study.

The propulsion system must provide power for the payload, the autopilot, control and communications systems, and for equipment cooling; a notable difference between the HI SPOT and HASPA specifications is that the HI SPOT payload requires 800 watts of electrical power, while the HASPA required only 200 watts. For our preliminary study, 200 additional watts of auxiliary power was assumed for onboard functions, for a total electrical power requirement of one kw. At low cruising speed these requirements exceed the power required for thrust, and the fuel required greatly reduces the endurance of a fueled vehicle.

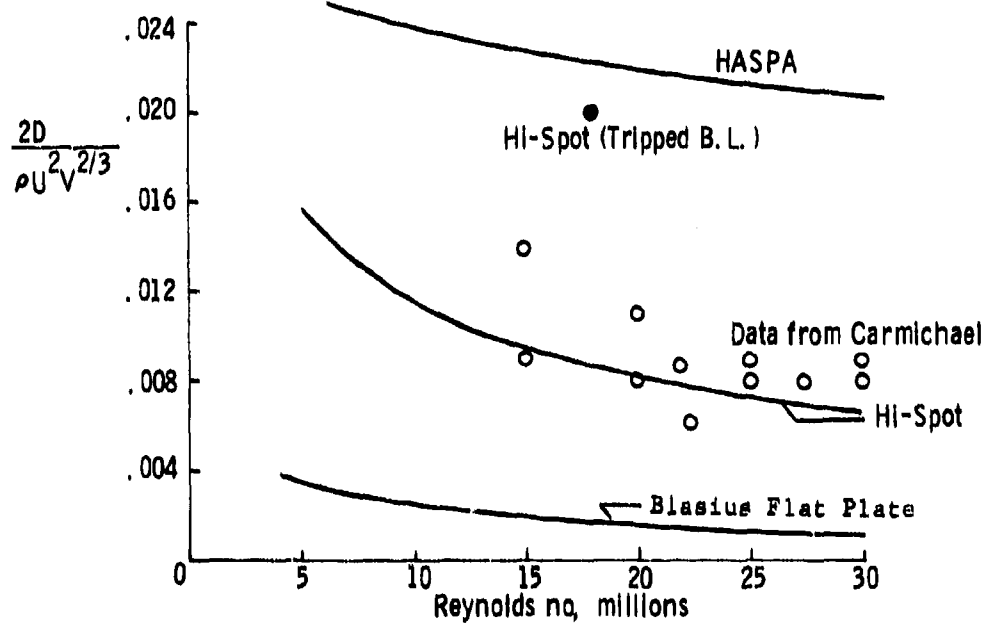


Figure 3: Comparison of Drag Coefficients

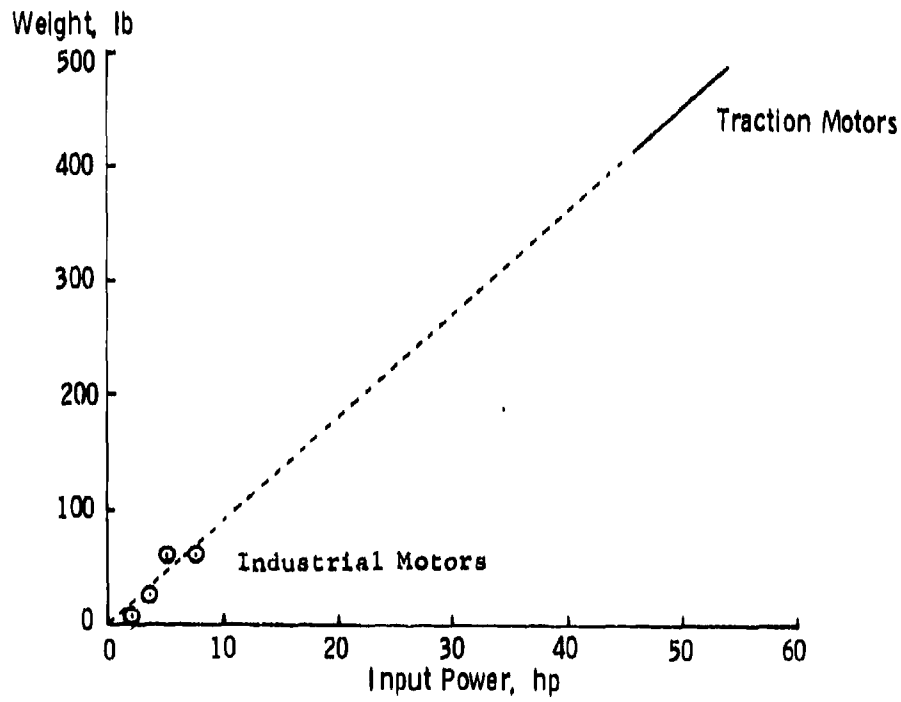


Figure 4: Electric Motor Weights

## Survey of Propulsion System Types

A propulsion system consists of an energy storage system, an energy conversion system, and auxiliary functions; in the HASPA, a solar energy collection system was included to replenish the storage system during daylight operations. Table I lists various options for the primary elements of the system; we will discuss each of these elements and options in order.

### Energy Sources

Energy is stored on board the aerostat in the form of mass (fuel, batteries, fuel cells, etc.), which is converted to energy in the forms of electricity or heat by chemical reactions, then expelled overboard or retained as waste. Some reactions, notably those producing electricity, are reversible, and the storage system can be replenished in flight by converting solar energy or by electromagnetic radiation from the ground. Since this latter requires large transmitting antennas, unsuitable for over-water operations, it will not be considered here. There are, then, two primary energy storage options to be examined for the HI SPOT system:

- electrical storage - chemical batteries

- fuel cells

- chemical storage - monopropellant fuels

- bipropellant fuels

- fuels burned in air

Table II compares these options in terms of their inherent specific energies and their net output energies for representative conversion efficiencies. The first notable observation of Table II is that the energy obtained by using the atmosphere (21% oxygen) surrounding the aerostat is an order of magnitude higher than the energies obtainable by operating, as it were, in vacuum. The second notable observation is that conversion of heat to shaft work is much less efficient than the conversion of electricity; and the third observation is that, notwithstanding its lower efficiency, much more shaft work is obtainable from fuel burned in air than from an equivalent mass of stored electrical energy. The advantage of electrical systems, then, is their ability to recharge by absorbing external energy and thereby operate indefinitely, but there is always some duration limit below which expendable chemical fuel weighs less than the equivalent rechargeable system.

### Energy Sources

#### Fuels

Hydrocarbon (Liquid Gas)  
Hydrogen (Liquid & Gas)  
Monopropellants  
Bi-Propellants (Fuel + Oxidizer)

### Power Plants

Electrical Motors - ac vs dc  
Engines -  
Airbreathing/Turbocharged  
Reciprocating  
Turbine  
Stirling  
Steam (Rankine, Hybrid)

### Speed Reducers

Gear Box  
Cone/Ball  
Belt/Pulley  
Hydraulic -  
Wobble Plate  
High-Speed Pump/Low-Speed Motor

### Radio Isotopes

SNAP/RTG

Electrical -

Variable Frequency  
Variable Voltage

### Solar

Cells  
Boilers/Heaters

### Electrical

Storage Batteries  
Fuel Cells

Table I: Survey of Propulsion System Elements

Energy Source	Specific Energy Btu/lb*	Representative Output Shaft Efficiency, (%)	Shaft Specific Energy	
			Btu/lb	lb/hp-hr
Storage Batteries				
Silver - Zinc	190	80	152	16.74
Advanced Lithium	1000	80	800	3.18
Fuel Cell (LH <sub>2</sub> - LO <sub>2</sub> )	3300	80	2640	.964
Stored Chemical Fuel				
Monopropellant	1411	40	565	4.5
Bi-propellant	2500	40	1000	2.54
Airbreathing Engines				
Fuel: Gasoline	18450	30	5540	.460
Diesel	17860	33	5890	.432
Propane	17860	33	5890	.432
Liquid Hydrogen	23420	31	7280	.350

\*Energy Density Includes Tankage Allowance

Table II: Comparison of Energy Sources

In recent years, reciprocating engines have been demonstrated which use hydrogen as fuel. Although there are slight gains in cycle efficiency, the principal advantages of hydrogen are its extremely high heat of combustion, approximately 50,000 BTU/lb, and its ready combustion at the low ambient pressure of high altitude. This is mitigated, however, by the difficulty of containment: hydrogen is cryogenic, and even in its liquid state, is a relatively low-density material requiring a large storage volume and tankage weight approximately equal to the weight of the hydrogen stored. Thus, as shown in Table II, the effective energy storage of hydrogen fuel is reduced from 50,000 BTU/lb. to about 23,000 BTU/lb.; this is an appreciable advantage over hydrocarbon fuels which average only about 18,000 BTU/lb. (including tankage allowances).

#### Electrical Energy Conversion

Converting electricity to rotary motion requires a motor and a speed controller. Generally, dc systems are simpler and lighter than ac systems, especially where the source is dc. As with other types of motors, high power-to-weight ratios are obtained by operating at high rotational speed; for a given power, motor weight tends to be inversely proportional to speed. Output speed and power are easily controlled by varying the applied voltage; a wide range of speed-torque characteristics are available.

Figure 4 is a representative sample of dc motor and controller weights over the range of power levels; the straight line is the expression used in the parametric aerostat sizing program. These weights represent current iron-copper motor technology; advanced concepts such as samarium-cobalt, electronic commutation, etc., have not been considered, though such technology is expected to be readily available in the early 1980's.

#### Heat Energy Conversion

Heat engines can be classified by their motion, by their thermodynamic working cycle, and whether the cycle is open or closed. For rotational speeds up to 8,000-15,000 rpm, reciprocating piston engines are most common, converting their motion to rotation by an eccentric crank; where higher speeds are acceptable and light weight is paramount, rotating turbines are generally used. Open-cycle engines use the hot gases resulting from the combustion process as a working fluid, exhausting the gas overboard as it is produced and used, while closed-cycle engines use a fixed quantity of

fluid which is heated and cooled through its thermodynamic cycle by heat exchangers. Figure 5 compares several of the more highly-developed cycles (Ref. 3).

The Carnot cycle is a theoretical cycle consisting of isentropic compression, heat addition at constant temperature, isentropic expansion, and heat rejection at constant temperature. The importance of this cycle is that it is, in theory, the most efficient cycle possible between the upper and lower temperature extremes. For example, a gasoline engine operating on a Carnot cycle, with a flame temperature of, say,  $2800^{\circ}\text{F}$  and a heat-rejection temperature of  $100^{\circ}\text{F}$  would have a cycle efficiency of 82%, corresponding to a specific fuel consumption of .167 pounds per horsepower hour, or about three times more efficient than a good automobile engine.

Both the Stirling and Rankine cycles are capable of Carnot-like efficiencies and are generally found as closed-cycle systems. The Rankine cycle, with various refinements, is commonly used in steam powerplants, and is highly developed in large sizes; while NASA and the Department of Energy are committed to the development of an automotive engine based on the Stirling cycle in the next few years. Both these cycles employ relatively heavy heaters and coolers, and are therefore not competitive where light weight is a criterion. For long endurance, however, fuel consumption dominates, and these engines can have significantly lower fuel consumption than internal combustion engines. The low ambient temperature and pressure at high altitude are particularly advantageous to the Rankine cycle, permitting cycle efficiency approaching 50%, which from Table II is equivalent to a hydrocarbon sfc of less than .316/HP-hr., or about 0.2 lb/HP-hr. using hydrogen fuel, and over a wide power output range.

Figure 6 presents estimated specific weights and fuel consumption of turbine driven closed Rankine cycle systems, including burners, boilers, condensers, and high-speed alternator/rectifier auxiliary power output, as well as turbines. These weights were estimated by analysis based on overall heat transfer coefficients of  $5 \text{ BTU/hr/ft}^2/^{\circ}\text{F}$  and other data obtained from Ref. 4. Because the specific weight increases rapidly for cycle efficiency above 40%-45%, the 40% value was selected for the aerostat sizing investigation.

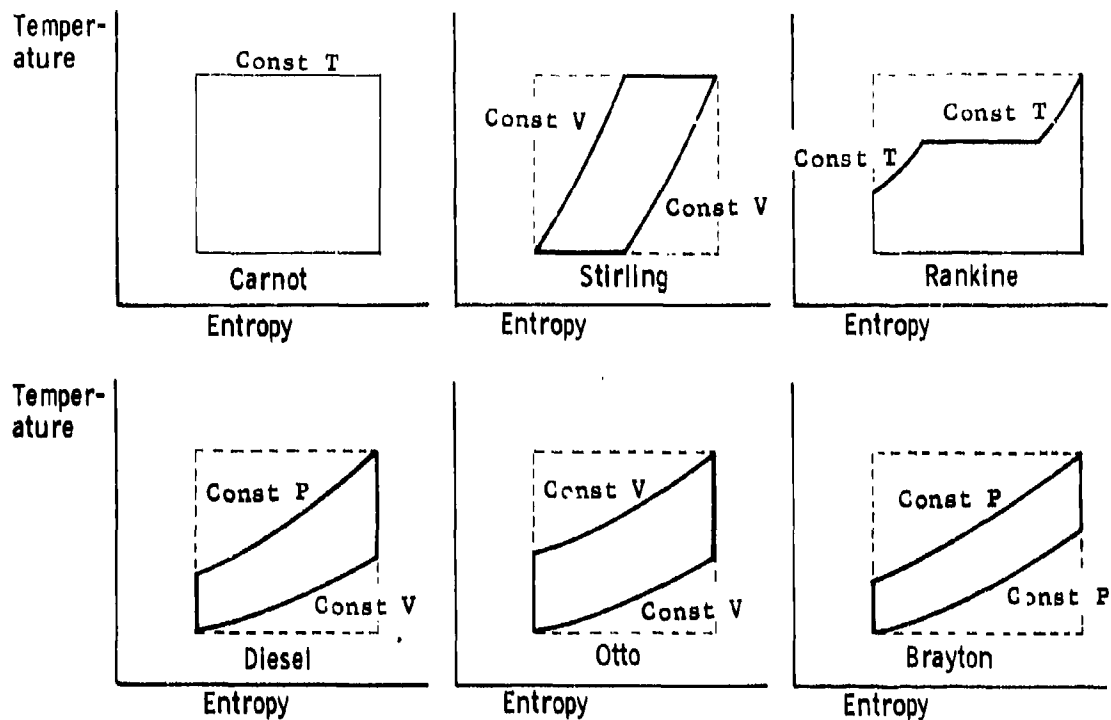


Figure 5: Comparison of Thermodynamic Cycles

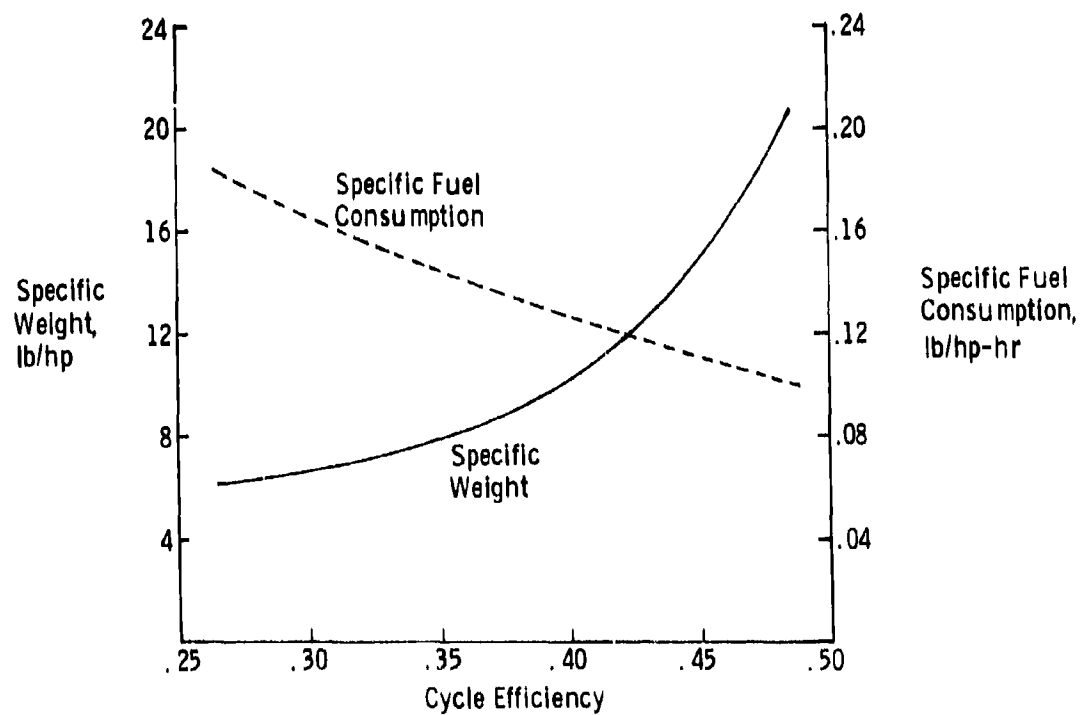


Figure 6: Hydrogen-Fueled Steam Turbine Characteristics

The internal combustion engine has seen its highest forms of development in the Diesel, Otto (spark ignition) and Brayton (gas turbine) systems. All of these are within a few percentage points of efficiency, though the Brayton engine is generally less efficient than the others and loses efficiency very rapidly at off-optimum conditions. The Diesel is usually more efficient than the Otto, but is also heavier and in the 5-50 HP range is primarily available as stationary engines with constant power output. However, automotive engines in this range are developing rapidly, with fuel consumption improvements of 10%-20%.

Since the power output of an airbreathing engine is proportional to the density of the air it ingests, supercharging is necessary to achieve reasonable power at high altitude. The technology of exhaust-driven turbosuperchargers is active and well-developed, and requires but minor extension to achieve the 10-15 manifold compression ratio required for engine operation at 50,000-70,000 feet. The single-stage turbosuperchargers used on current aircraft, such as the Beechcraft Duke, Mooney 231, and Piper Lance, achieve compression ratios of 5; it is therefore apparent that dual stages would be required. However, there is ample energy available in the exhaust gas: the isentropic compression ratio achievable in expanding from a typical exhaust temperature of  $1600^{\circ}\text{F}$  ( $2060^{\circ}\text{R}$ ) to  $100^{\circ}\text{F}$  ( $560^{\circ}\text{F}$ ) is 95 to 1, while expanding and compressing at 70% efficiency (49% overall) results in an exhaust gas temperature of  $775^{\circ}\text{R}$  ( $315^{\circ}\text{F}$ ) for a compression ratio of 15. Additional study is required to determine whether currently available hardware can be adapted to multiple-stage turbocharging or whether new impellers and compressors would need to be developed. Figure 7 presents representative weight and power data on turbosupercharged reciprocating engines, obtained from Ref. 5. The dashed curve is an exponential correlation of these data, and the solid curve includes a 20% allowance for a more complex starting system and for cooling shrouds and fans; the equation shown was used to determine powerplant weights for the aerostat sizing program (Appendix "B").

The turbocharged diesel engine obtains lower fuel consumption than the spark-ignition engine at the expense of higher engine weight, and is therefore superior for long-endurance applications. However, this is a relatively flat tradeoff, and because the compression-ignition cycle is also less suitable for hydrogen fuel than spark ignition, diesels have been largely ignored in this study.

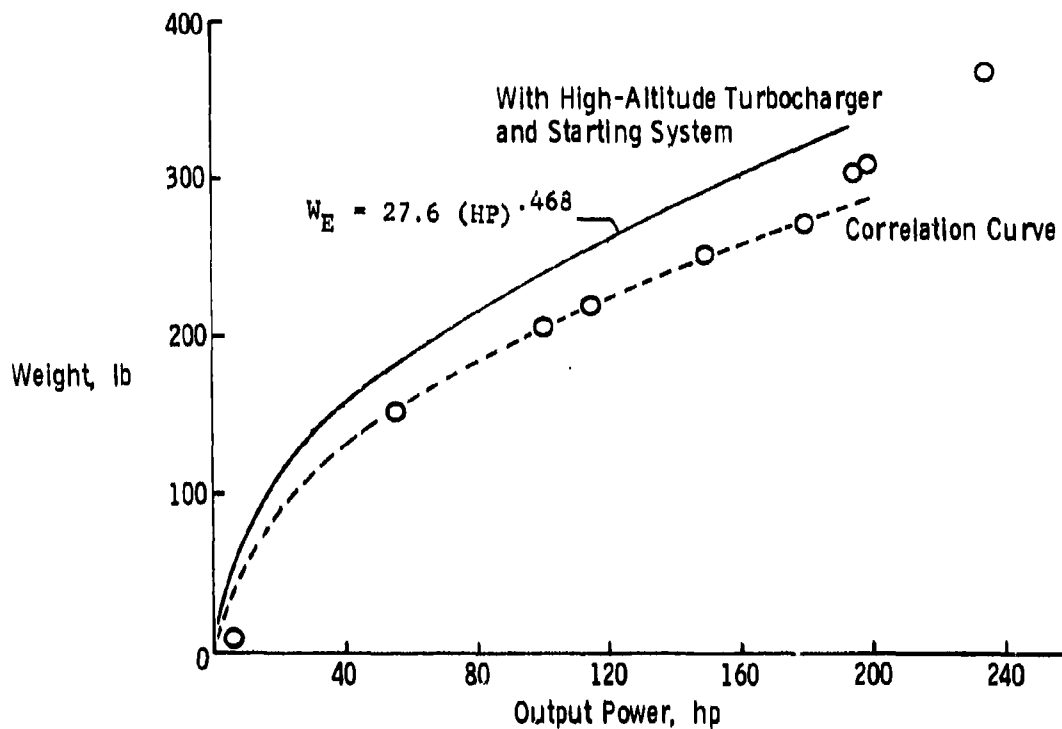


Figure 7: Weights of Reciprocating Engines

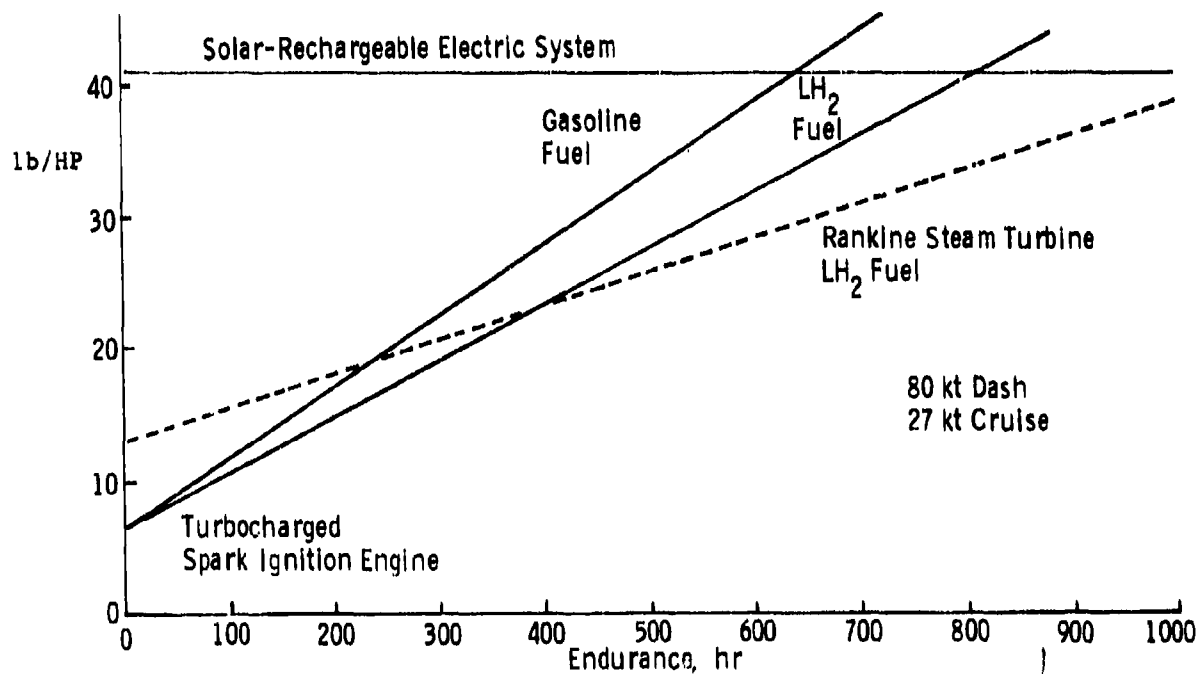


Figure 8: Comparison of Propulsion Systems

Two-stroke cycle engines are generally much lighter than four-stroke cycle engines of the same power. However, their fuel consumption is approximately double that of the four-stroke, they lose efficiency more rapidly at off-design conditions, and they must be mechanically supercharged because their efficiency is very sensitive to exhaust back pressure. These engines are only suitable for mission durations up to 100-200 hours because of their high specific fuel consumption.

The ultimate lightweight engine is the gas turbine, or Brayton cycle engine. However, while good specific fuel consumption can be obtained at design output, the partial-power sfc deteriorates very rapidly, and gas turbines are therefore not suitable in applications where most of the operating time is at very low power settings as in the HI SPOT. Another disadvantage of gas turbines is their high rotation speed (up to 100,000 rpm in small sizes); this requires larger speed reductions and therefore heavier weights to match the engine to the propeller.

Brayton cycle engines are available in either open-cycle or closed-cycle systems. The Airesearch Corporation, for example, produces both types as auxiliary power units. The open cycle is, of course, the lightest, while the closed cycle has the advantage of using non-oxidizing working fluid and thereby operating at higher maximum temperatures to achieve improved efficiency. However, a closed Brayton cycle system is generally less efficient than a closed Rankine cycle system of equal weight, and has therefore not been considered further.

In summary, three propulsion concepts were selected for the comparative aerostat sizing task:

1. A turbocharged, gasoline-fueled, spark ignition engine
2. A closed, hydrogen-fueled, Rankine cycle turbine engine
3. A solar-cell, regenerative fuel cell, dc motor system

#### Comparison of Propulsion Systems

As shown in Fig. 1, an aerostat with a speed range of 20 to 60 kt must operate at power settings as low as 5% of maximum; as will be shown later, average operating power is 20% or less. The advantage of a fuel-burning system over a heavy, constant weight system is best illustrated by examining an artificial parameter, the installed-power specific fuel consumption,

defined as the average fuel flow rate divided by the maximum installed power. Thus, a spark-ignition engine having an average sfc over its power range of 0.6 lb/HP-hr. would have an installed-power sfc of .06 if operated at 10% average power; .12 at 20% average power, and so on. This enables a very simple comparison of the weights of different powerplants, as shown in Figure 8 for an electric cell system, a Rankine cycle system, and a turbo-charged spark-ignition system, all designed for 100 kt dash speed with 28 kt average speed. The electric cell system is heaviest, but since it collects and stores solar energy, it requires no fuel, and its endurance is unlimited, or more properly, is indefinite. The spark-ignition engine is lightest, but its fuel consumption makes the system weight equal the weight of the rechargeable system at 650 to 800 hours, depending on whether gasoline or hydrogen is used as fuel. Intermediate is the Rankine steam-turbine system; though the engine installation is nearly twice as heavy as the reciprocating engine, its fuel efficiency is half again as good, and it is superior in total weight at endurances from 400 to 1100 hours.

### Propellers

The ideal location for an airship propeller is at its stern: properly tailored to the wake diameter and velocity distribution, a stern propeller could restore the wake to freestream velocity and thereby approach 100% propulsive efficiency (neglecting the fin and gondola wakes and the energy losses of the propeller itself). However, the stern mounting has several disadvantages:

1. The overhanging weight of the propeller and mount system produces undesirable bending stresses in the envelope;
2. Long wire runs are required between the central control gondola and the stern mount, resulting in electrical losses and a weight penalty.
3. The two widely separated masses of the central gondola and a stern propulsion module increase the complexity of the launch and handling procedures.

4. The gondola and the propulsion module represent much of the cost of the system, and efforts to recover them are warranted. However, if these modules are separated, as with a stern propeller, the recovery procedure is more difficult and expensive than if recovered as a unit.

It is considered that these disadvantages outweigh the efficiency advantages of the stern location, and a gondola-located propeller has been assumed for this study.

As shown in Reference 6, propeller weight is proportional to the product (power)<sup>1/3</sup> (Diameter)<sup>4/3</sup>, with the proportionality factor determined by the propeller material and construction. Power required is determined by the aerostat drag coefficient and speed, while diameter is determined by the efficiency desired:

$$D_p^2 = \frac{N_1^2}{1-N_1} \frac{C_D V^{2/3}}{\Pi}$$

where  $N_1$  is the ideal momentum efficiency of the propeller. For advance ratios near unity, good propellers achieve at least 90% of their ideal efficiency (Ref. 6), and assuming an overall propeller efficiency of 85% results in the following equations:

$$D_p = .960 \sqrt{C_D} L$$

$$N_p = 112.5 V/D_p$$

where the symbols are as defined in Appendix "B". Figure 9 is a carpet-plot of propeller speed as functions of the aerostat drag coefficient and the aerostat speed parameter  $V/L$ . The important point to be noted, however, is that efficient propellers for low speed operation must be large in diameter and must operate at hundreds, not thousands, of rpm; this dictates that speed reducers must be used to match optimized propellers to optimized engines.

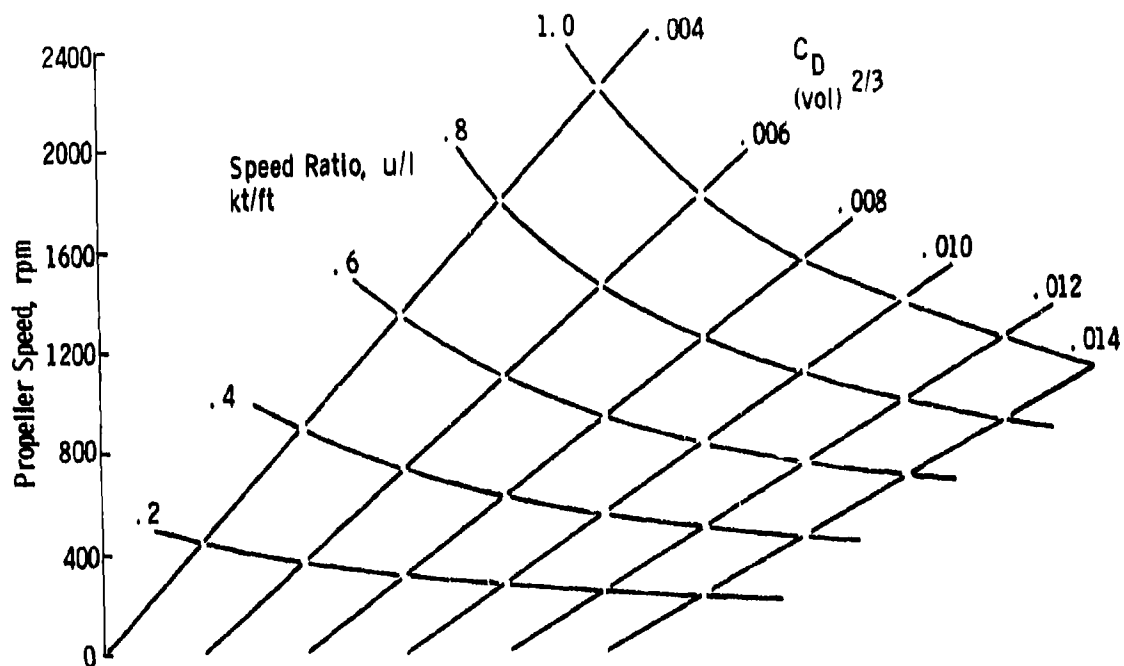


Figure 9: Aerostat Propeller Speeds at 85% Efficiency

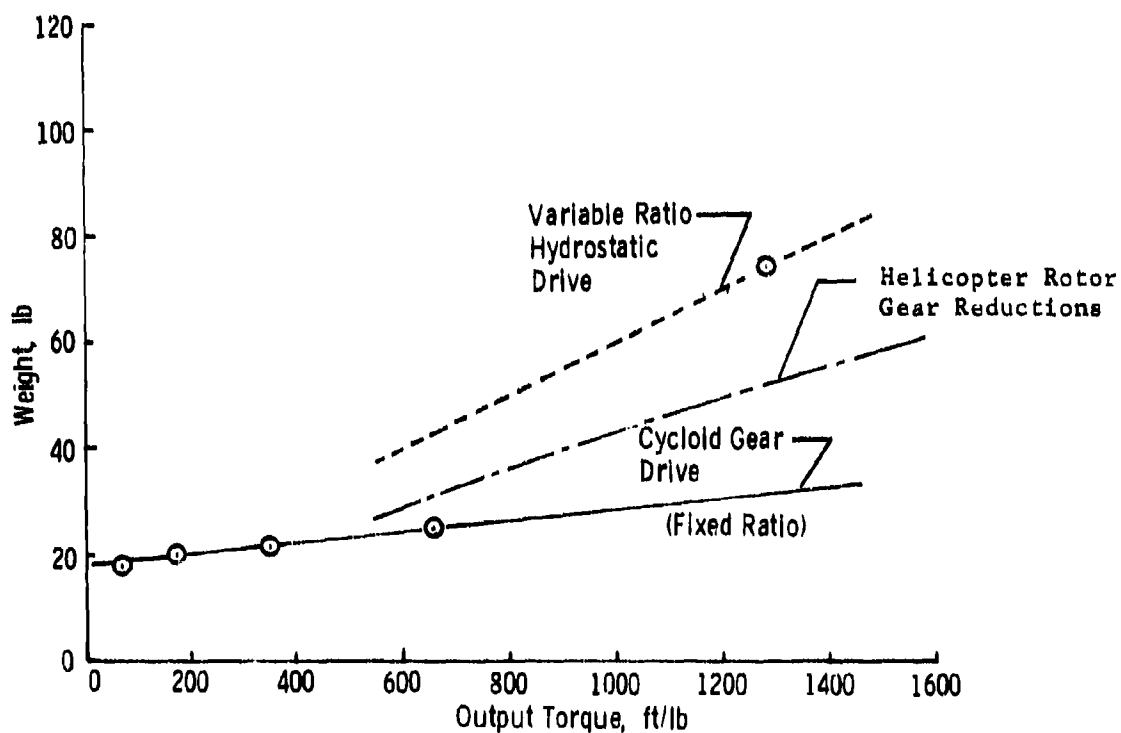


Figure 10: Weights of Speed Reducers

## Speed Reducers

Two ranges of speed reducers are required: for reciprocating engines, order-of-magnitude speed reductions are required; and for turbine-drive systems, the reduction ratio must be about two orders of magnitude.

There are three basic ways to achieve a reduction in rotation speed: mechanical, electrical, or hydraulic; each has advantages and disadvantages.

**Mechanical Reductions.** Mechanical reduction system subclassify as geared, belted, or chain-driven and as single-stage or compound (multiple-stage); there are also combined systems, and several varieties of geared systems. As a class, all of these systems are roughly comparable in efficiency, weight, and reliability for a given power and reduction ratio. Single-stage efficiency up to 98% is obtainable at reduction ratios up to 1/5; since two to four stages of reduction are required for the HI SPOT, efficiencies range from 90% to 95%. The gear system weight is dominated by the output torque required, as shown in Figure 10, which compares geared reductions with hydrostatic oil pump and motor sets. (Data obtained from References 7-9).

**Hydraulic Reduction.** Reduction gearing provides a fixed ratio of output speed to input speed, and requires a precise geometric alignment between the input and output. In contrast, a hydraulic pump and motor set can be operated over a wide range of input/output ratios and with no constraints on their relative positions, alignments, or motions. Also, the motor can be tailored to produce a wide range of speed-torque characteristics for matching to the expected load and is readily controlled, including stopping and restarting. The penalty paid for this versatility is weight, as shown in Figure 10; the variable-ratio hydrostatic system requires 50%-100% more weight than an equivalent gear reduction system.

**Electric Speed Reduction.** A miniaturized alternator, driven at high speed, can provide rectified dc power to drive a relatively slow-speed motor, thus providing a high degree of speed reduction between the power source and the drive unit. This type of drive is widely used for aircraft accessory drives, such as wing flaps, landing gear, etc. However, the torque obtainable from an electromotive force across the necessary air gap between a stator and a rotor is considerably less than that obtainable from meshing gears, and it is readily verified that at hundreds of rpm, an electric motor with an integral gear reduction is considerably lighter than a low-speed motor.

Summary. Mechanical gearing is probably the lightest and most efficient means of reducing the high speed of a motor or turbine to the speed required for an efficient aerostat propeller. However, the mechanical system requires precise alignment between the motor and propeller, and the rigid coupling provides a ready path for unwanted vibrations and oscillations; it also requires that the input speed be varied in order to change the output speed. In contrast, a hydrostatic drive system renders the input and output shafts independent of each other in terms of both speed and spatial relation. At slow motion especially, the hydraulic motor is considerably lighter than an electric motor. Finally, hydraulic fluid is a ready means of transferring and dissipating the heat produced by the inefficiencies of the system. For these reasons, the hydrostatic drive system was selected for the aerostat sizing study.

#### Summary of Propulsion Technology Assessment

In summary, a high altitude powered aerostat based on the Navy Class C hull would require impossibly high power to maintain station in winds exceeding 50-60 knots, but lower-drag hull forms are available which would permit speeds in excess of 100 knots. A solar-rechargeable fuel cell system weighs tens of pounds per horsepower; replacing this system with a lightweight airbreathing engine provides fuel capacity for hundreds of hours of operation before the engine and fuel system equals the weight of the regenerative fuel cell-solar cell system.

The ideal fuel is hydrogen, due to its ready ignition and its very high heat of combustion; its advantages are reduced but not eliminated by the weight of the cryogenic containment system required. However, as exemplified by their widespread use and high state of development, gasoline and diesel fuels are acceptable alternatives, possessing the advantages of higher density and easy handling and storage.

Two engine types were selected for parametric study: a turbocharged, spark-ignition, reciprocating engine and a Rankine-cycle steam turbine engine. The reciprocating engine was selected as the lightest-weight, most highly developed system in the 5-50 HP power range, and the Rankine steam cycle was selected for its low fuel consumption potential at a weight intermediate to the solar-cell/fuel-cell system and the spark-ignition system.

Large diameter, slow-turning propellers are required for good efficiency in the HI SPOT speed/altitude regime. The analytical and structural technologies required are well developed; however, the large size results in propeller weight approaching the engine weight. In addition, a speed-reducing system is required to reduce the engine speed to the propeller speed; again, this system equals or exceeds the engine weight. Reduction gearing is highly efficient and lighter than a hydrostatic pump and motor system; but the hydrostatic system is more versatile and vibration free.

### Parametric Comparison of Aerostats

#### Introduction

The purpose of the propulsion technology assessment was to define parametric equations for a comparison of the effects of the propulsion system on aerostat size. While it is illuminating to consider the performance of a given aerostat with different types of powerplants, it is more significant to compare aerostats of equal performance, with their sizes determined by the characteristics of the various powerplants, as this gives a truer picture of the complexity, cost, and operational comparisons that should be considered in addition to the performance. All non-propulsion elements are held constant: the hull shape and fineness ratio, fin areas, hull material, control system, auxiliary equipment, and so on. This section presents and discusses the sizes of powered aerostats having two types of airbreathing propulsion systems, and compares these with the original HASPA and with a low-drag, solar-rechargeable, electrically propelled configuration.

#### Winds

While the overall wind at the 50 mb pressure level in the middle latitudes of the northern hemisphere averages about 16 knots, this average is not randomly distributed, either seasonally or spatially. The seasonal variation is extreme, with the day-to-day average wind changing by approximately a factor of three from winter to summer, and a 1%-2% expectation of winter wind speeds at certain locations exceeding 6 times the year-round average. In order to assure a high probability of station-keeping mission success, the Navy has provided the two winter wind frequency distributions presented in Figure 11 for design purposes, representing two areas currently

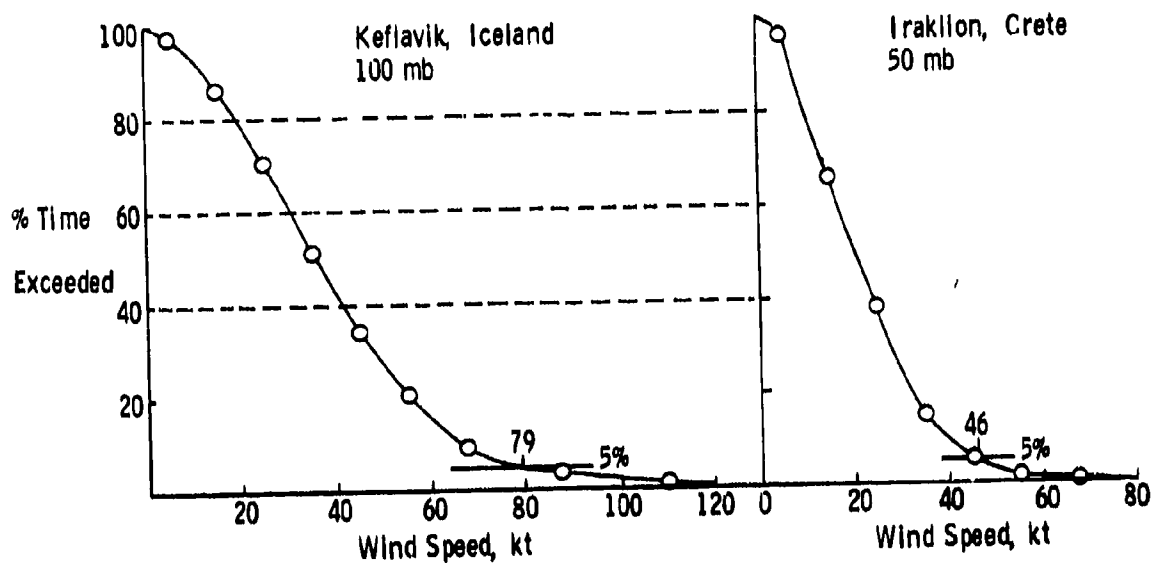


Figure 11: Upper Atmosphere Winds

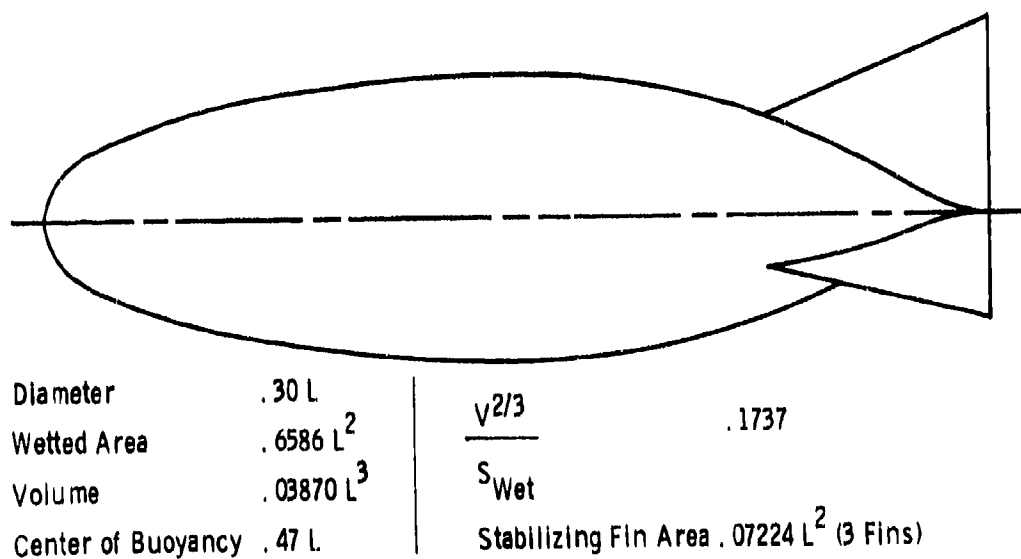


Figure 12: NACA 67030 Profile Characteristics

of interest for over-the-horizon surveillance. The HI SPOT aerostats are sized to achieve 30 days endurance against these wind profiles, with a maximum speed capability equal to the highest wind expected for 95% of the time; this guarantees a better than 98% probability of remaining on-station for 30 days or more the year around.

Because the thrust power required varies approximately as speed cubed, the fuel consumed over a 30-day interval corresponds to the power required for a speed considerably higher than the mean wind. Integrating the curve of thrust power required and computing the airspeed corresponding to the average power results in the power-average speeds indicated on Figure 11. These are about 59% of the maximum speed for each profile.

#### Aerostat Characteristics

Based on Carmichael's high Reynolds number drag experiments, a hull shape based on a NACA 67030 laminar-flow airfoil profile is chosen for all configurations. Figure 12 lists the geometric characteristics of this shape in parametric form, and also includes the fin area required to stabilize the hull in pitch and yaw, based on a correlation of the tail lengths and areas of several successful airships. The engine, propeller, payload, and other subsystems are carried in a single low-drag gondola suspended below the aerostat at its center of buoyancy. The fins are fixed, with directional control provided by yawing the propeller from side to side to control the aerostat heading. This scheme confines all wiring and control systems within the gondola and thereby reduces weight. Analyses of this control system have shown that, though sluggish, it is more than adequate to maintain the aerostat within its required 50 n.m. station-keeping radius (Appendix "A").

A controlled valve in the hull releasing helium as fuel is used in order to limit the internal pressure to a safe value during the mission.

Figure 13 is a carpet-plot of the volume required to lift an aerostat to the altitudes shown, based on helium of 99% purity. This plot is independent of the hull shape; however, the right hand scale indicates the lengths of the NACA 67030 hull shapes required to provide these volumes.

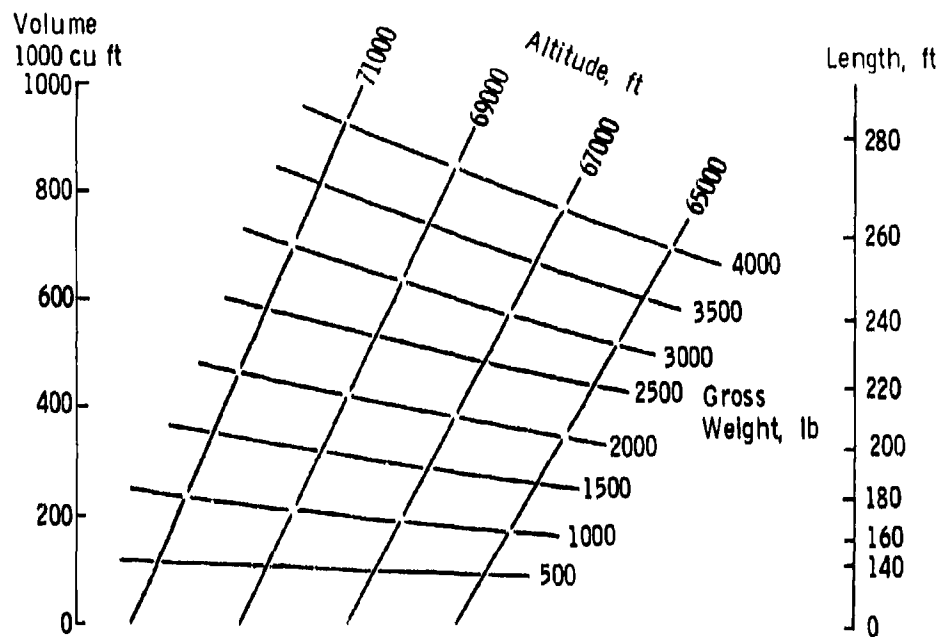


Figure 13: Aerostat Volume and Length

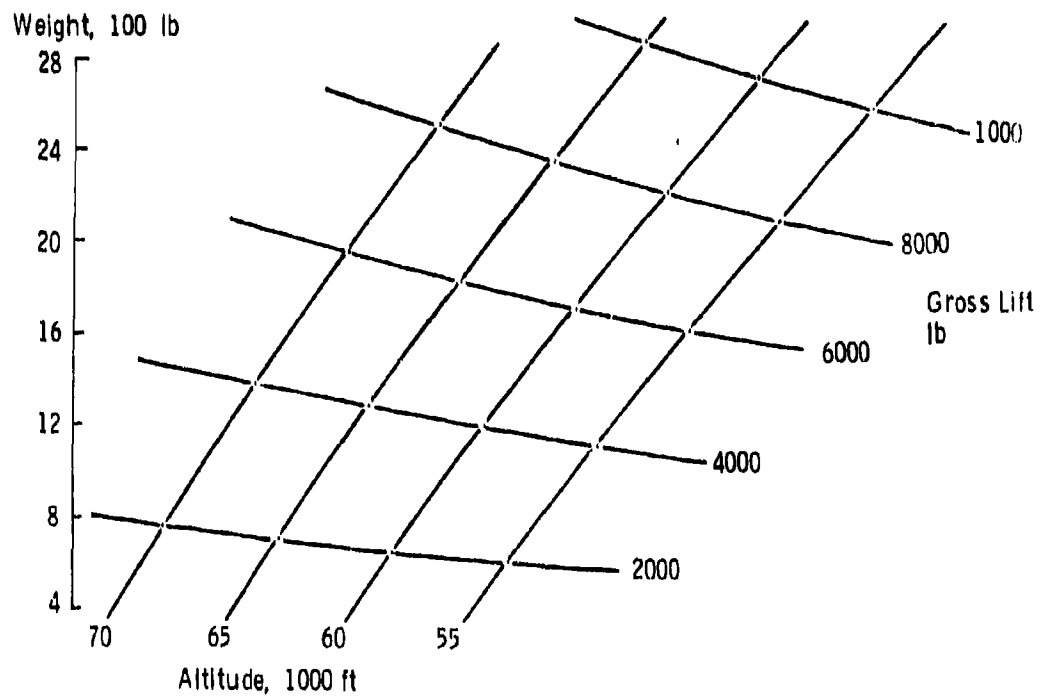


Figure 14: Weight of Aerostat Hull and Fins

A Kevlar 49 scrim bonded to a film of aluminized mylar is assumed for the hull structure. For simplicity, a uniform scrim, based on the strength required at the maximum hull diameter and bending moment, is assumed. The required strength is determined by first determining the minimum internal pressure required to prevent aerostat buckling under load, and from that pressure determining the maximum design pressure resulting from diurnal heating of the fixed mass and volume of enclosed gas. Because only two or three percent of the design pressure is determined by the bending moment, pressure required is dominated by the design altitude, and the influence of size is negligible.

Limited data obtained during the HASPA program indicated that under long-term loading, Kevlar 49 may fail at loads as low as 50% of its quick-break strength. Assuming this, and allowing a design limit strength  $2/3$  of the long-term ultimate strength, results in a design working strength  $1/3$  of the 405,000 psi advertised ultimate strength of Kevlar 49. Using hoop and longitudinal loads estimated at the maximum diameter of the aerostat, the required mass of Kevlar per square foot is determined, added to the mass per square foot of aluminized mylar gas barrier and adhesive, multiplied by the wetted area of the hull to determine the hull weight, and multiplied again by 122% to account for overlapping seams, reinforcing patches, and the fin area, as shown in Appendix "B". Figure 14 presents the estimated structure (hull and fin) weights as functions of gross lift and altitude. The difference between the gross lift and the structure weight represents the weight available for lift gas, propulsion system, subsystems, and payload. It can be seen that weight of structure required for a given lift capacity increases only slightly with altitude, even though the volume required increases in proportion to the density decrease; this is because the design pressure, and therefore the weight of Kevlar required for a given volume, decreases with increasing altitude.

As already noted, the HI SPOT aerostat must have a substantial speed capability to be sure of keeping station under adverse conditions, even though it may cruise at only 15-20 knots for much of the year. For the inverse square-root drag function shown in Figure 3, Figure 15 shows the aerostat thrust power required as functions of weight and airspeed. It is of interest to note that the  $1/\sqrt{R_0}$  drag function eliminates the density

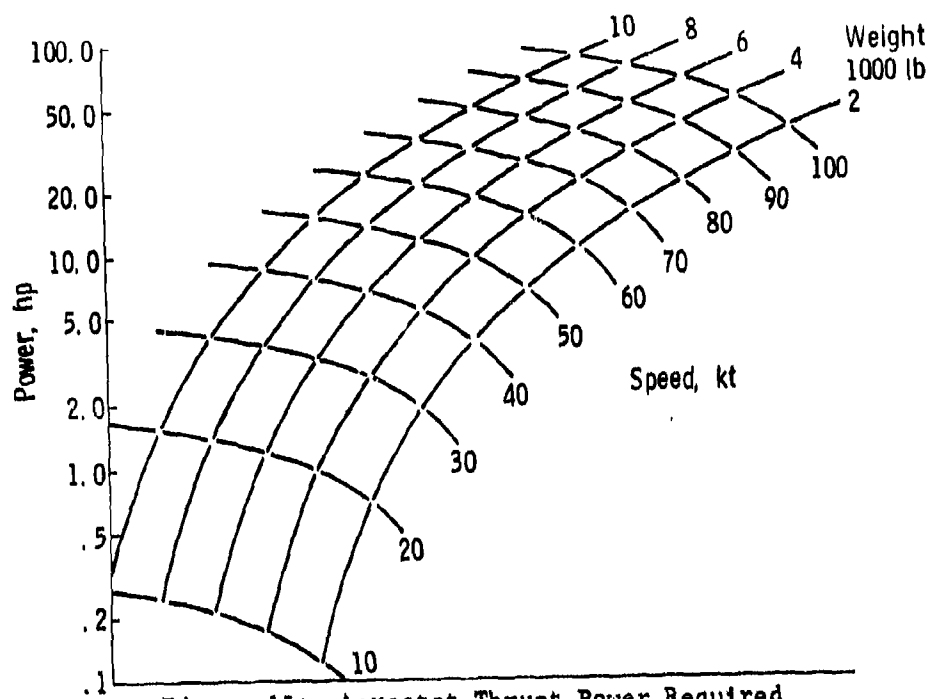


Figure 15: Aerostat Thrust Power Required

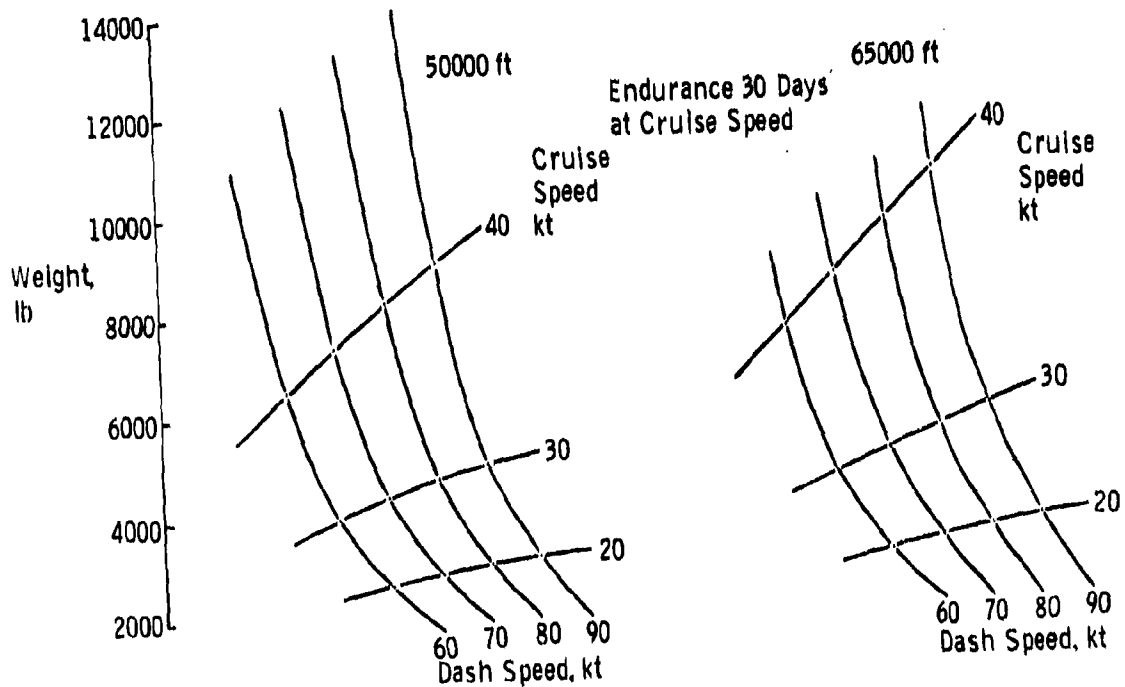


Figure 16: Weights of Turbocharged Spark-Ignition Systems

from the power equation, producing the simple function,  $P = \sqrt{WU^5} / 116800$  (horsepower, given the weight, W, in pounds and the speed, U, in knots). For determining powerplant size, these values must be corrected for propeller and reduction drive efficiencies, then added to the 1000 watt (1.34 HP) auxiliary power requirement; note that at low speeds, the auxiliary power exceeds the thrust power required.

### Powerplant Characteristics

The parametric study uses equations for closed-cycle steam turbine and turbocharged reciprocating engine weights derived from the data presented in Figures 7 and 8 (see Appendix "B"). To compare these engines with a solar-cell/fuel cell system, data from Reference 10 were used.

Current technology in solar arrays yields approximately 125 watts/lb for a cell oriented toward the sun; assuming that four times as many cells as this must be used to permit the aerostat heading to be independent of the solar direction and latitude reduces the yield to 31 watts/lb, which converts to 23.88 lb/HP. Similarly, an advanced regenerative hydrogen-oxygen fuel cell now under development (but not available for several years, Ref. 10) will produce 190 watt-hours per pound, equivalent to 3.93 lb/HP-hr; assuming a 10 hour charge, 14-hour discharge cycle, the fuel cell must weigh 55.0 lb/HP. (This is considerably lighter than the 385 lb, 19.5 HP-hr Apollo fuel cell envisioned for HASPA I.) Because the fuel cell operates for an assumed 14-hour period, it is sized to provide the power represented by the power-average cruise speed while the solar array provides the power required at maximum speed. Three conditions can therefore be envisioned during which the solar-regenerative aerostat is inadequately powered: daytime at speeds near maximum, when the solar cell output is insufficient to both propel the aerostat and recharge the fuel cell; nighttime when the average wind speed exceeds the design cruise speed long enough to deplete the charge on the fuel cell, and wintertime at high latitude when the day/night cycle is unbalanced more than the assumed 4 hr toward the night side and average solar radiation is inadequate to provide power for both recharging and high average speed.

### Subsystems, Payload, and Reserves

Besides the powerplant itself, the aerostat must incorporate a reduction drive, propeller, fuel system, control and autopilot system, command/communications transceiver, pressure valve, equipment cooling, the payload, and a gondola in which to house all this. Also, the gross volume includes the helium which pressurizes the hull, and allowance must be made for errors and omissions resulting from the simplified parametric equations presented in Appendix "B". Propellers and reduction drives have already been discussed, and parametric data for their weights have been derived. Assuming liquid hydrocarbon fuel, the fuel containment and distribution system is assumed as  $1/25$  of the fuel weight (typical for unpressurized aluminum tanks; for cryogenic hydrogen, the containment system is taken as 1.135 times the hydrogen weight (insulated/Dewar tank system). As a rough approximation, and following normal aircraft practice, all other equipment is taken as weighing 40 lb plus  $1/20$  of the engine, reduction drive, and payload weight (representing controls and cooling systems), plus the 200 lb payload itself. HASPA (Ship No. 2, battery powered) carried avionics weighing 187 lb, plus 257 lb of recovery parachute, dc/ac converters, equipment cooling system, and power distribution system. However, as an engineering development vehicle, the avionics included both a ground-commanded autopilot and an automatic navigation system, as well as engineering instrumentation and telemetering equipment. These weights are therefore considered as excessive for an operational design. Also, it is considered that the large reinforced box framework of the HASPA gondola is not appropriate to an operational vehicle design. For sizing purposes, therefore, aluminum monocoque construction is assumed, and the gondola weight is assumed as 20 lb for shock attenuation and miscellaneous provisions plus  $1/25$  of the propulsion, subsystems, and payload weights allowed for the structural shell, attach points, and suspension system.

Finally, 10% of all weight except the helium and fuel is reserved (added) as a contingency allowance for unforeseen growth and to guarantee an identifiable conservatism in the results to be presented.

### Results of Parametric Sizing

Using the equations presented in Appendix "B", aerostat size has been determined for 30 days endurance at altitudes of 50,000 and 65,000 feet for a matrix of cruise and dash speed capabilities and for aerostats with reciprocating airbreathing engines, Rankine steam turbine engines, and solar-rechargeable electric systems. Carpet-plot results are presented in Figures 16, 17, and 18. The airbreathing systems are much more sensitive to cruise speed requirements than to maximum speed, while the solar-rechargeable system is about equally sensitive to either. At low speeds, all configurations seem to be comparable, while at high cruise speeds, the rechargeable systems appear smaller. For all powerplant types, increasing the design altitude increases the gross lift required to achieve the desired performance. This is because the reduced density requires a larger and heavier hull to carry a given equipment weight.

Figure 19 compares the three types of aerostat systems sized to achieve the same performance, with maximum speed as the variable; the HASPA aerostat is also included. The HASPA vehicle, resized to benefit from up-to-date materials, solar cell, and fuel cell technologies, would still require excessive size to carry a payload at speeds above 45-50 knots. Introducing the low-drag hull configuration, but retaining the indefinite-endurance propulsion system, still requires a 9,300 lb gross weight (approximately  $2.3 \times 10^6 \text{ ft}^3$ ) for a 100-knot speed capability, at which weight a reciprocating engine vehicle would have nearly 1200 hours (50 days) endurance, and a steam-turbine vehicle would have 88 days endurance at cruise speeds. However, note that for maximum design speeds less than about 80 knots, the indefinite-endurance configurations are substantially lighter than the fuel-burning configurations, and since this is in the speed range of the wind distributions used, would satisfy year-round station keeping requirements over much of the northern hemisphere. At higher latitudes, however, large increases in solar cell capacity would be required to offset the low solar angle and unbalanced day-night cycle; this would cancel out the weight advantage of the solar-rechargeable system.

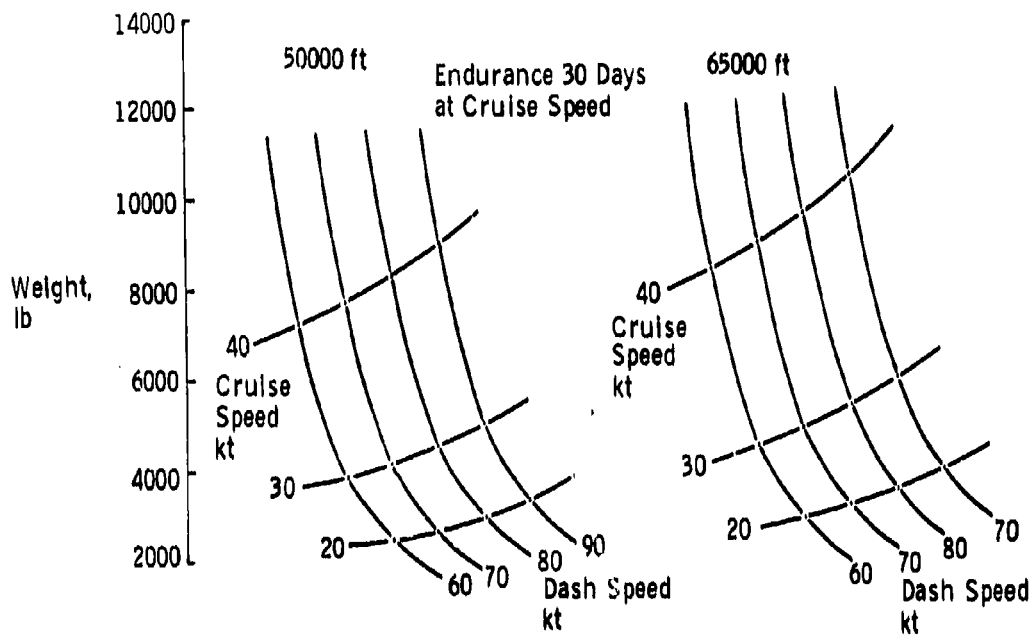


Figure 17: Weights of Hydrogen-Fueled Steam Turbine Systems

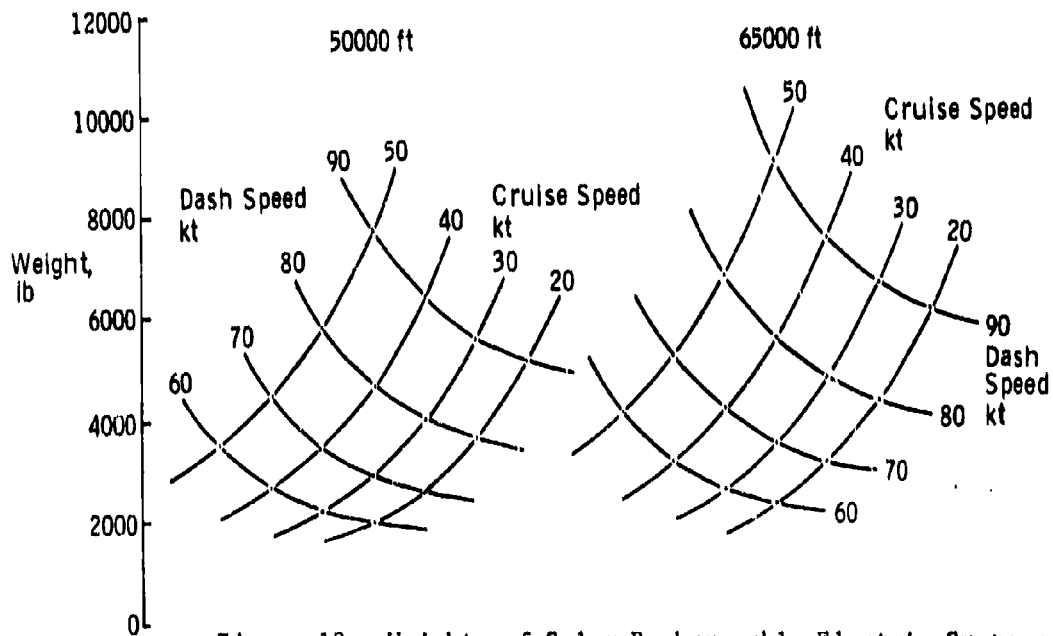


Figure 18: Weights of Solar-Rechargeable Electric Systems

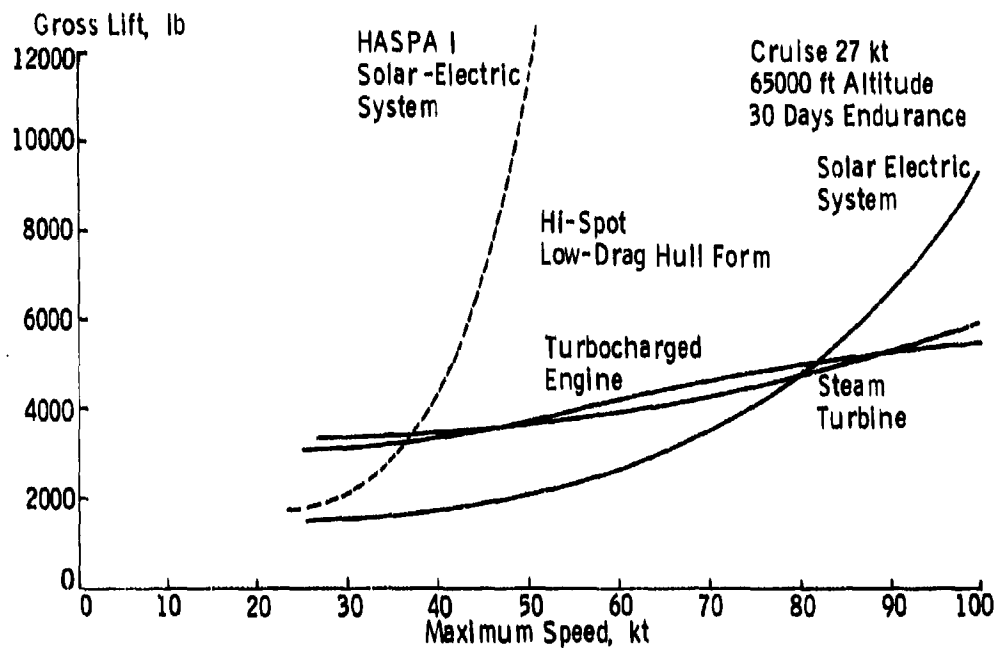


Figure 19: Influence of Maximum Speed on Gross Lift Required

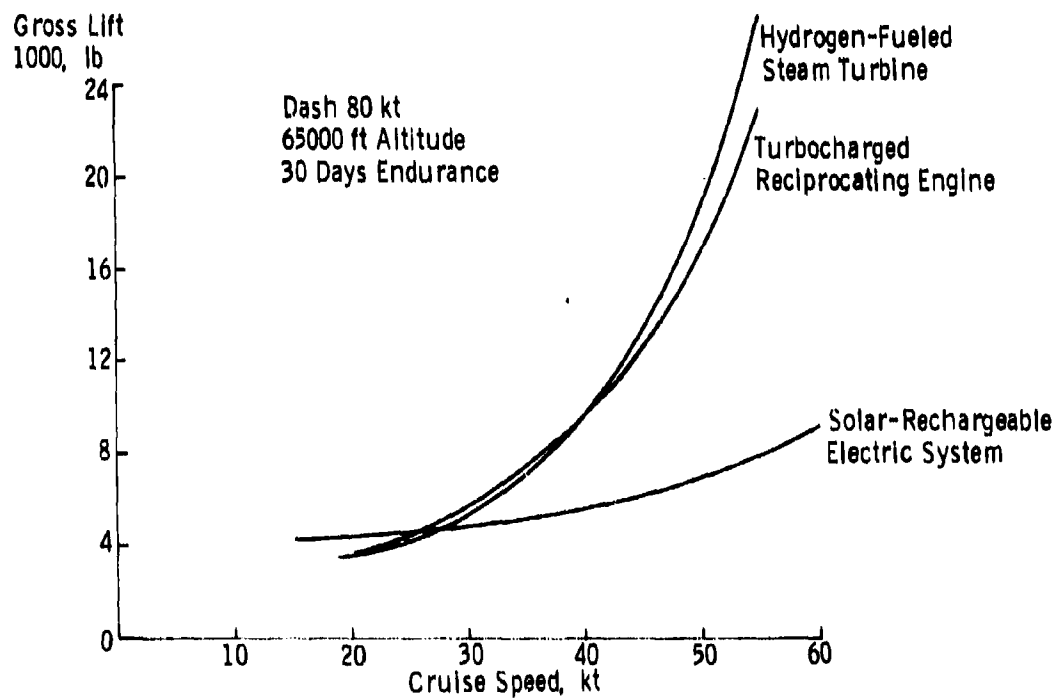


Figure 20: Influence of Average Cruise Speed on Gross Lift Required

Figure 20 compares aerostats with the three types of propulsion systems in terms of cruise speed, all with 80 kt maximum speed capability. In this case, the lighter configurations are found to be the fueled systems, at cruise speeds below 27 kt, and the solar-rechargeable system at higher cruise speeds; the fueled systems are much more sensitive to increasing speed requirements (for 30 days endurance) than is the solar-rechargeable system. Finally, Figure 21 compares the endurance of two equal-size aerostats (800,000 ft<sup>3</sup>, 3,930 lb gross lift) as functions of cruise speed. Each aerostat has a 39.5 HP powerplant giving it a dash capability of 79 kt. Both configurations are quite comparable, with the turbocharged, gasoline engine having about a 2-day endurance advantage at all speeds. As can be inferred from Fig. 20, a solar-rechargeable configuration with these speed capabilities is virtually the same size.

In general, the lightest vehicles are the solar-rechargeable electric systems; the fueled systems are lighter only if the maximum speed is greater than about 80 knots, or if the ratio of the maximum to cruise speeds is large (3 or more). However, there are other factors to consider.

First, the installation, checkout, and launch in a limp state of several thousand square feet of solar cells is an enormous, labor-intensive task, and would probably require that the aerostat be launched in an inflated, pressurized condition to achieve satisfactory operation. Second, the regenerative fuel cell must be charged with liquid hydrogen, thus requiring cryogenic storage and handling at the launch site. (This is true also for the hydrogen-fueled airbreathers). Third, additional solar cell capacity must be carried if the aerostat is to operate at high latitudes, and additional fuel cell capacity is required for an unbalanced day/night cycle; these factors diminish or even eliminate the weight advantage.

On the other hand, the fueled systems are confined entirely within the gondola and require no circuitry, sensors, or controls on the envelope other than the pressure control valve, and they can operate throughout their speed range independent of place and time of day. Moreover, a gasoline-fueled vehicle requires about 500 lb of gasoline just to provide the 800 watts of payload power for 30 days; an inert payload of 700 lb could therefore be carried as easily as the 200 lb, 800 watt payload by simply offloading fuel.

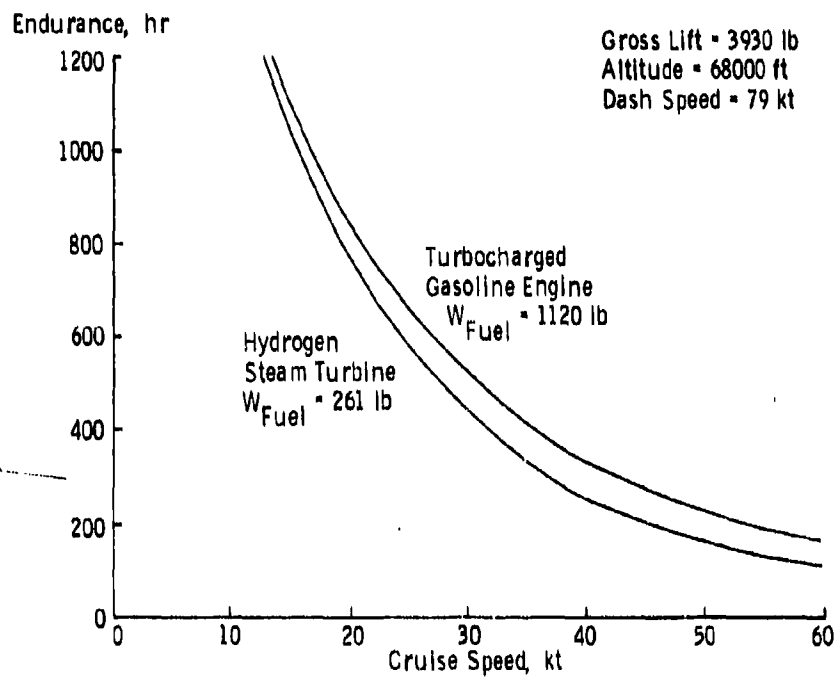


Figure 21: Influence of Average Cruise Speed on Endurance

The endurance of the fuel users can also be increased by loading more fuel: the weight-carrying capacity of an 800,000 ft<sup>3</sup> envelope is 3,930 lb at 68,000 ft, 4,540 lb at 65,000 ft, and a whopping 9,370 lb at 50,000 ft. Of course, some of this weight must be used to reinforce the hull against the higher pressures it must sustain, and to increase the power so that the design speeds can be attained. Nevertheless, the air-breathing vehicle has a broader, more flexible range of operating conditions than the solar-rechargeable system.

In summary, the solar-rechargeable system is lighter, but more complex to construct and handle, and less flexible in its operating parameters, than is the airbreather. Finally, accepting the complexity of a hull-mounted solar collection system, the fuel consumption of a steam turbine system could be halved by employing solar heaters to heat the condenser water to as much as 300°F, using fuel only for the final heating stages.

#### Conclusions

In conclusion, we have found that adequate technology now exists to build high altitude aerostats with speed capabilities as high as 100 knots, either with solar-rechargeable fuel cells having indefinite endurance, or with airbreathing combustion engines having limited endurance but great flexibility of operations and simplified systems. The principal achievement of this study, other than the assessment of propulsion technology, is the application of low drag hull forms having laminar-like drag coefficients to the high altitude, station keeping aerostat.

The most promising propulsion system studied is the steam turbine system, possessing an energy conversion efficiency of at least 40% and capable of improving to as much as 70% with solar heating.

Technology is currently available to assemble a gasoline-fueled, turbocharged reciprocating engine to power a lightweight aerostat with a speed capability of 100 knots and 30 days endurance against northern hemisphere winter winds. Technology advancements projected for the next 5-10 years, but not discussed in this report, can improve this performance substantially. Similar advancements projected for electric motors and controllers in this time period will result in large weight reductions in solar-rechargeable systems as well.

### Cited References

1. Carmichael, B.H., "Underwater Vehicle Drag Reduction Through Choice of Shape," AIAA Paper 66-657, Jun 1966.
2. Schlichting, H., "Boundary Layer Theory," 6th Ed, 1968.
3. Lee, J.F., and Sears, F.W., "Thermodynamics," 1956.
4. Martin, C.G., (Energy Technology, Inc., Cleveland, Oh), "Steam Boiler and Condenser Relations," Private communication to W. L. Marcy, Jun 1979.
5. Aviation Week, "Aerospace Inventory Edition," March 12, 1979.
6. United Aircraft Corp, Hamilton Standard Division, "Generalized Method of Propeller Performance Estimation," Report PDB6101, Jun 1963.
7. Machine Design, "Mechanical Drives Reference Issue," Dec 1969.
8. Mangum, J. E. (Bell Helicopter Div, Textron, Inc., Ft. Worth, TX), "Helicopter Gearbox Weight Estimating," Private communication to W. L. Marcy, Jun 1979.
9. Machine Design, "Fluid Power Reference Issue," Sept 1970.
10. General Electric Co., Aircraft Systems Div, "Primary Fuel Cell System for HASPA 30 Day Mission," Briefing presented to W. L. Marcy, Martin Marietta Corp., Jan 1979.

APPENDIX "A"  
CONTROL STUDIES  
R. O. Hookway

Hi-Spot Control Concepts

The Hi-Spot control system must meet a very simple requirement: The aerostat must remain within 50 nautical miles of its designated station. This requires that the aerostat possess a heading control, a speed control, a navigation or tracking system, and a logic circuit to vary these parameters in the presence of changing wind speed and direction.

Heading control is provided by vectoring the thrust axis in the direction of travel desired and allowing the weathercock stability of the hull/fin combination to null out the resulting sideslip. This confines the control, sensor, and power circuitry to the gondola, and thereby simplifies the hull, reduces weight, and eases the fabrication, checkout, and launch procedures. The principal disadvantage of this system is that, because the aerostat thrust/weight ratio is only about 1/100, the turning force available is rather small, the maximum rate of turn is therefore slow, and the minimum turning radius about 5 n.m. However, this is only 1/10 of the maneuvering space available, and station-keeping should therefore be no problem.

Previous studies have shown that a bang-bang control system containing predictive logic makes more efficient use of the relatively low control forces available for dirigible flight control. In the bang-bang configuration, when appropriate control force is needed the propeller is driven in the proper direction to its maximum position at the maximum gimbal rate, whereas with a linear system the propeller slowly returns from the extreme commanded position to lesser deflections until control errors are nulled. The comparison of the response to the two control laws is shown in Figures A-1 and A-2.

The bang-bang predictive control logic is most easily described with reference

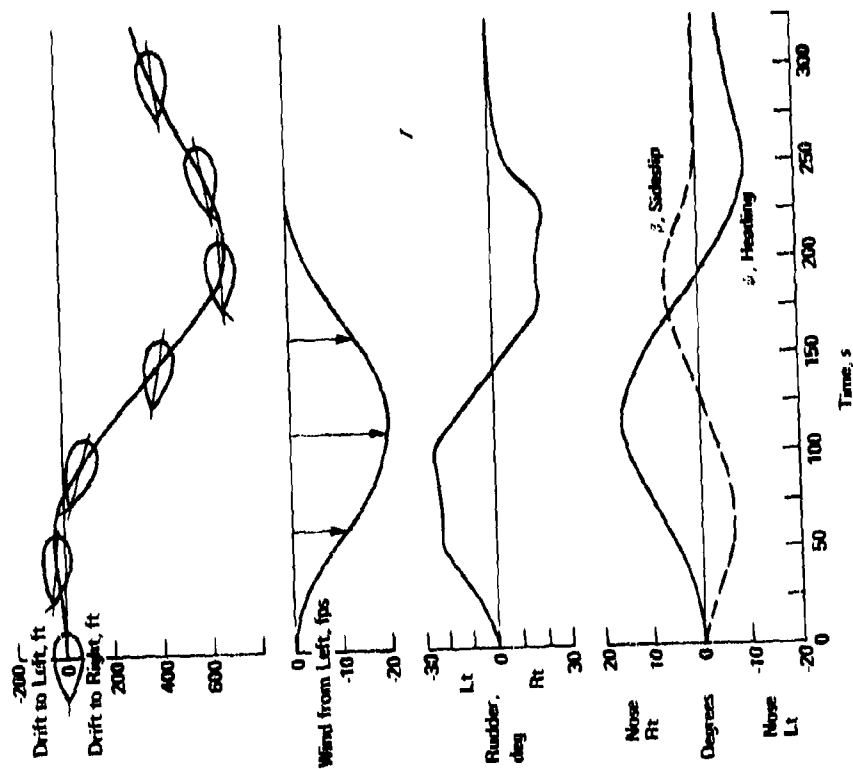


Figure A1: Response to Wind (Linear Control Law)

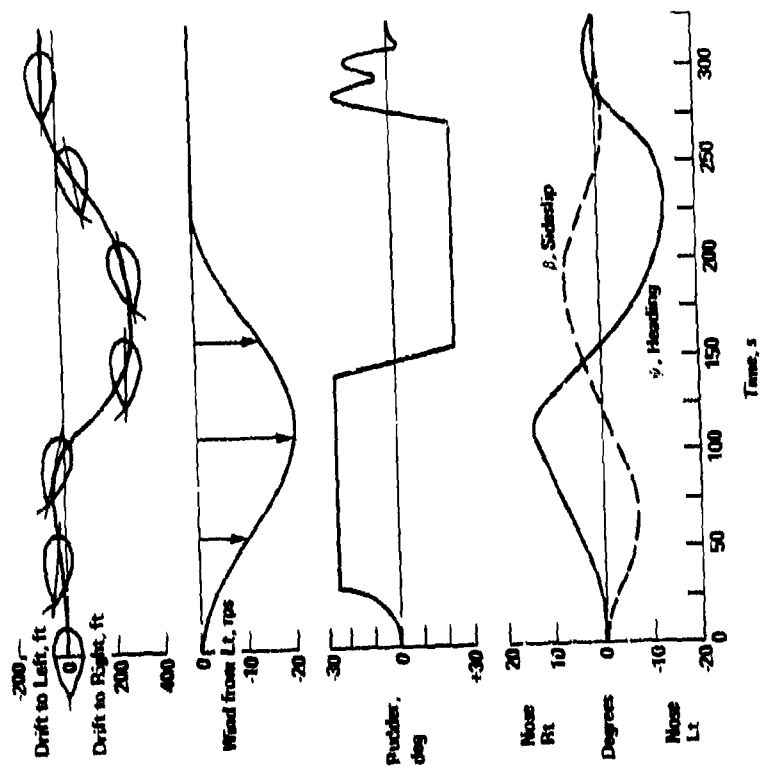


Figure A2: Response to Wind (Fastcom Control Law)

to the phase plane of Figure A-3. If the initial conditions are such that  $\psi_E$  and  $\dot{\psi}_E$  are of the same sign (1st or 3rd quadrants), the gimbal deflection ( $\delta_y$ ) is driven to its stop in the direction to make  $\delta_y$  the same sign as  $\psi_E$ . This drives the phase plane trajectory into the 2nd or 4th quadrant respectively as shown in Figure A-3. In order to drive the trajectory to  $\psi_E = \dot{\psi}_E = 0$  (synchronization), the control force must be reversed at the conditions ( $b$ ). The control reversal condition is determined by predictive logic in the flight controls computer, which predicts in fast time (hence, we call the control law Fastcom) where the trajectory will go if the gimbal is reversed at, say, ( $A_2$ ). Since the predicted trajectory for this condition does not achieve synchronization, another test is made at ( $b_2$ ). The predicted trajectory from ( $b_2$ ) does achieve synchronization and so ( $b_2$ ) is the proper time to switch control polarity. The locus of switching points ( $b$ ) is a unique function of the characteristic of the aerostat; the locus shown in Figure A-3 is for a dirigible of 200,000 ft<sup>3</sup> volume with a stern mounted propeller.

The bang-bang nature of Fastcom is advantageous because it makes maximum use of the available control force, but it tends to limit cycle after completion of the basic maneuver. This limit cycling is eliminated by switching to a linear control law when the trajectory crosses a switching boundary. When the trajectory is outside of the boundary the system uses the predictive logic, and when the trajectory is inside the boundary the linear control law is used.

#### AIRSHIP DYNAMICS

To study the effects of configuration changes, linearized perturbation equations in turning moment and side force were used. The inputs required for the equations include:

- . aerodynamic coefficients:  $C_{n_B}$ ,  $C_{n_F}$ ,  $C_{y_F}$ ,  $C_{y_B}$
- . mass properties: physical mass (including helium)

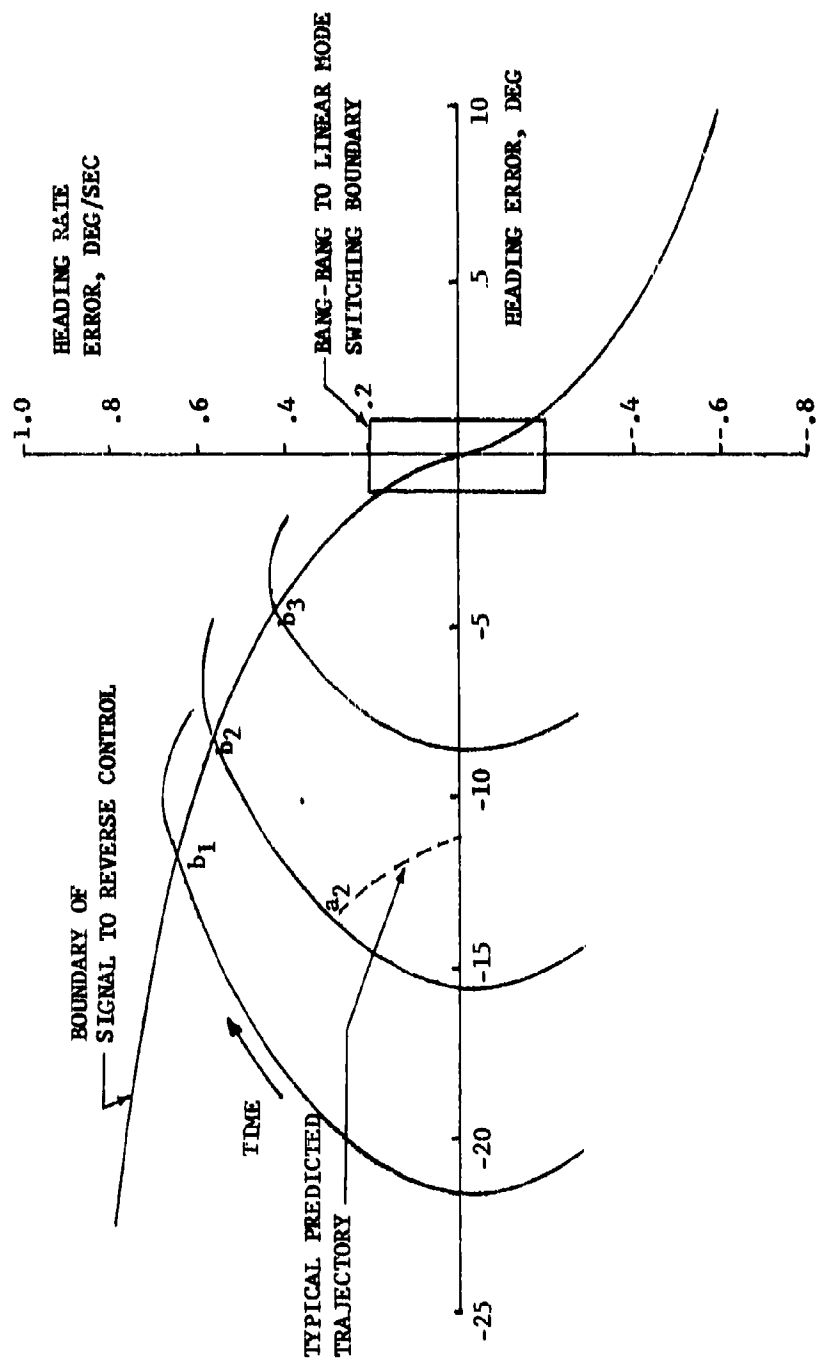


Figure A3: FASTCOM Control Law Performance

apparent mass

physical inertia about yaw axis

apparent inertia about yaw axis

Table A-1 presents the aerodynamic coefficients and dimensional force, moment, and damping derivatives estimated for three different aerostat sizes. These derivatives were estimated by theoretical and empirical methods from several sources, and would need to be verified and corrected to more accurate values during the development of an actual aerostat.

To evaluate the controllability of various Hi-Spot configurations, several flight events were simulated:

- 1) Response of Hi-Spot to a sidewind while the controls are locked to show its weathercock stability.
- 2) Ability of Hi-Spot to drive initial errors in heading and heading rate to zero in still air (shows functioning of Fastcom logic).
- 3) Lateral distance which Hi-Spot drifts off station in a typical wind while Fastcom is operating.
- 4) The response of Hi-Spot to a commanded 180 degree turn.

Weathercock stability is shown in the response of the 800,000 ft<sup>3</sup> Hi-Spot derigible to a 20 ft per sec step gust, Fig. A-4. In seven seconds, the airship has reached 63 percent of the final heading change caused by the wind input; the response is approximately 0.8 damped. These results show that the configuration has adequate directional stability without artificial damping or other active heading controls. However, as shown by comparing Figures A-4 and A-5, an active control system reduces the lateral drifts by approximately 37 percent from that experienced by the vehicle with its controls locked.

Figure A-5 shows the response of HISPOT when it is controlled by the Fastcom control law. The system produces near optimum performance (minimum time

Table A-1. HI SPOT Aerodynamic & Mass Properties Data

Column	1	2	3
Aero data source	MMC	MMC	MMC
Volume-ft <sup>3</sup>	200,000	800,000	912,000
F.R.	3.33	3.33	3.33
Length-ft	167	274.4	280
Dia-ft	40	82.33	84
Exposed area, 1 fin	715	1813	1978
Mass-slugs	31.2	180	205
Apparent mass-slugs	60.9	394	422.
$I_{ZZ}$ -sl ft <sup>2</sup>	98701.	1,493,000.	1,771,000.
$I_{ZZA}$ -sl ft <sup>2</sup>	113,500	1,527,000.	1,760,000.
$C_{n\beta}$	+0.363	+0.363	+0.363
$C_{y\beta}$	-2.166	-2.166	-2.166
$C_n$	-0.319	-0.319	-0.319
$C_{yr}$	+0.757	-0.757	-0.757
$N_\beta$	+0.1087	+0.1422	-0.3017
$Y_\beta$	-12.29	-25.65	-55.54
$N_r$	-0.3143	-0.3654	-0.5379
$Y_r$	-14.15	-26.21	-39.39
(1-Nr)	2.15	2.023	1.994
$U-Y_r$	11.19	20.72	29.61
$U(1-Y_{ij})$	74.77	149.65	211
$Y_\delta$	+0.071	0.2206	0.4556
U-ft/s	25.33	46.93	69.
h	60,000	60,000	60,000
$\rho$			

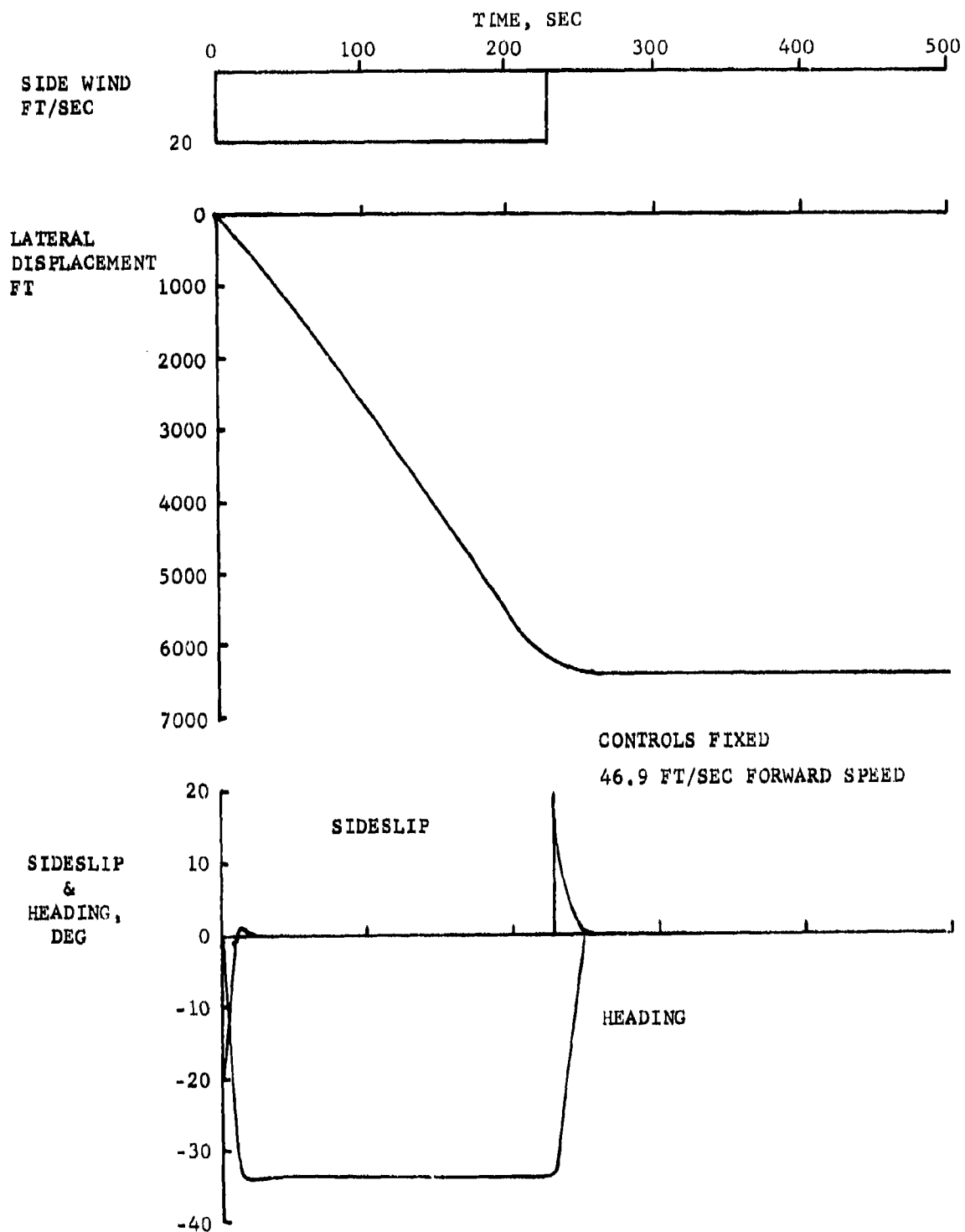


Figure A4: HI SPOT Airship Response to Side Wind

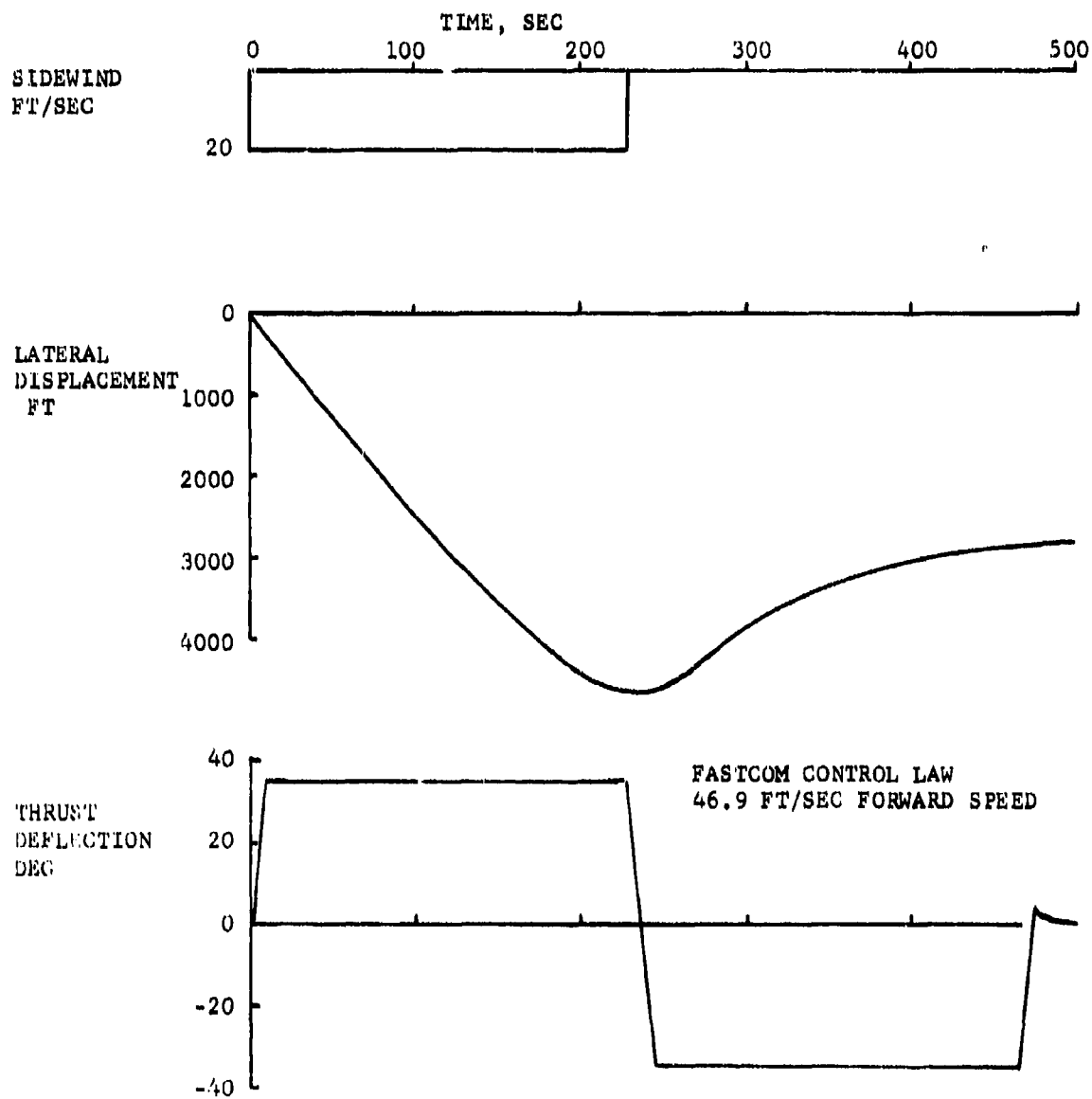


Figure A5: 800,000 Ft<sup>3</sup> HI SPOT Airship Response to Side Wind

to reach the mode switching boundary) in that only two control pulses are used. The overshoot in thrust deflection when heading error reaches 1 degree is due to low damping in the linear mode. The damping can be increased by straightforward changes in the control loop. Figure A-6 shows a 912,000 ft<sup>3</sup> dirigible responding to a 20 ft per sec step gust. Since the response is similar to that shown in Figure A-5 for an 800,000 ft<sup>3</sup> dirigible, the Fastcom control law is applicable to a broad range of aerostat sizes.

Finally, there is the need to evaluate the capability of maneuvering this class of dirigible by the use of Fastcom logic to drive the CG mounted propeller so as to execute turns within the specified 50 mile radius of a point on the ground.

The transfer function of turning rate ( $\Delta\dot{\psi}$ ) in response to rotation ( $\Delta\delta$ ) of the thrust direction around the vertical axis through the CG is given by:

$$\frac{\Delta\dot{\psi}}{\Delta\delta} = \frac{Y_{\delta} N_{\beta}}{[U_o(1-Y_{\dot{y}})(1-N_{\dot{x}})] s^2 - [(1-N_{\dot{x}}) Y_{\beta} + N_r U_o(1-Y_{\dot{y}})] s + N_r Y_{\beta} + N_{\beta}(U_o - Y_r)}$$

Inserting the derivatives for the 800,000 ft<sup>3</sup> HISPOT flying at 28 kt (46.9 ft/sec), the steady state turning rate becomes 0.0891 deg per sec, the turning radius is 30,141 ft (4.96 n mi), and the time to turn 180 degrees at 46.93 ft per sec (28 kts) is 2,017 secs (33.6 minutes). The radius and time to turn are large when compared with conventional dirigibles but are well within the mission requirements specified for HISPOT. A simulation of this turn is shown in Figure A-7.

While the HISPOT possesses good directional stability, it needs a heading control to keep it tracking accurately over the ground. This can be done in crude fashion by simply tracking the craft and commanding thrust vector changes from the ground, or in more sophisticated fashion by providing autonomous onboard

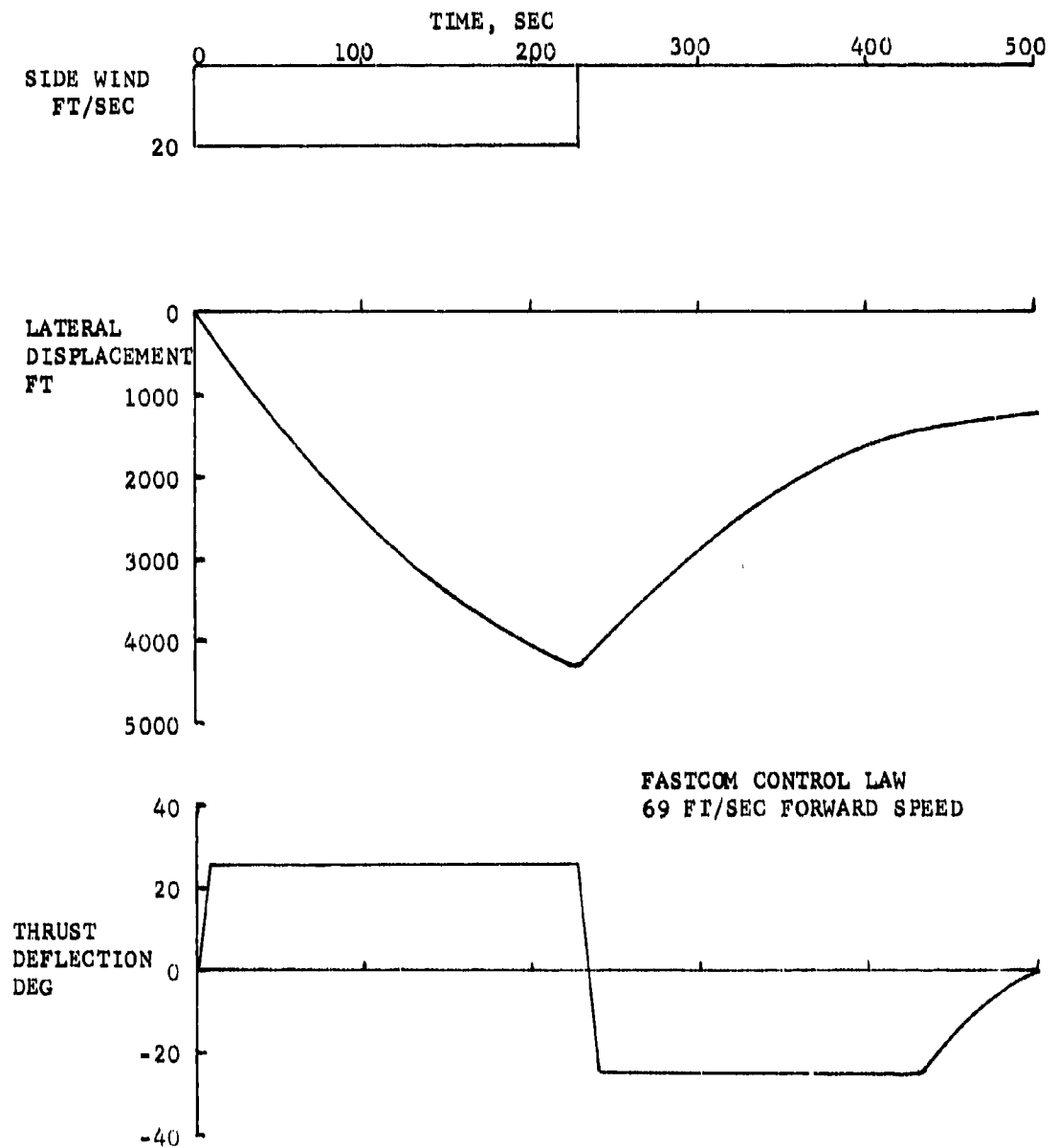


Figure A6: 912,000 Ft<sup>3</sup> HI SPOT Airship Response to Side Wind

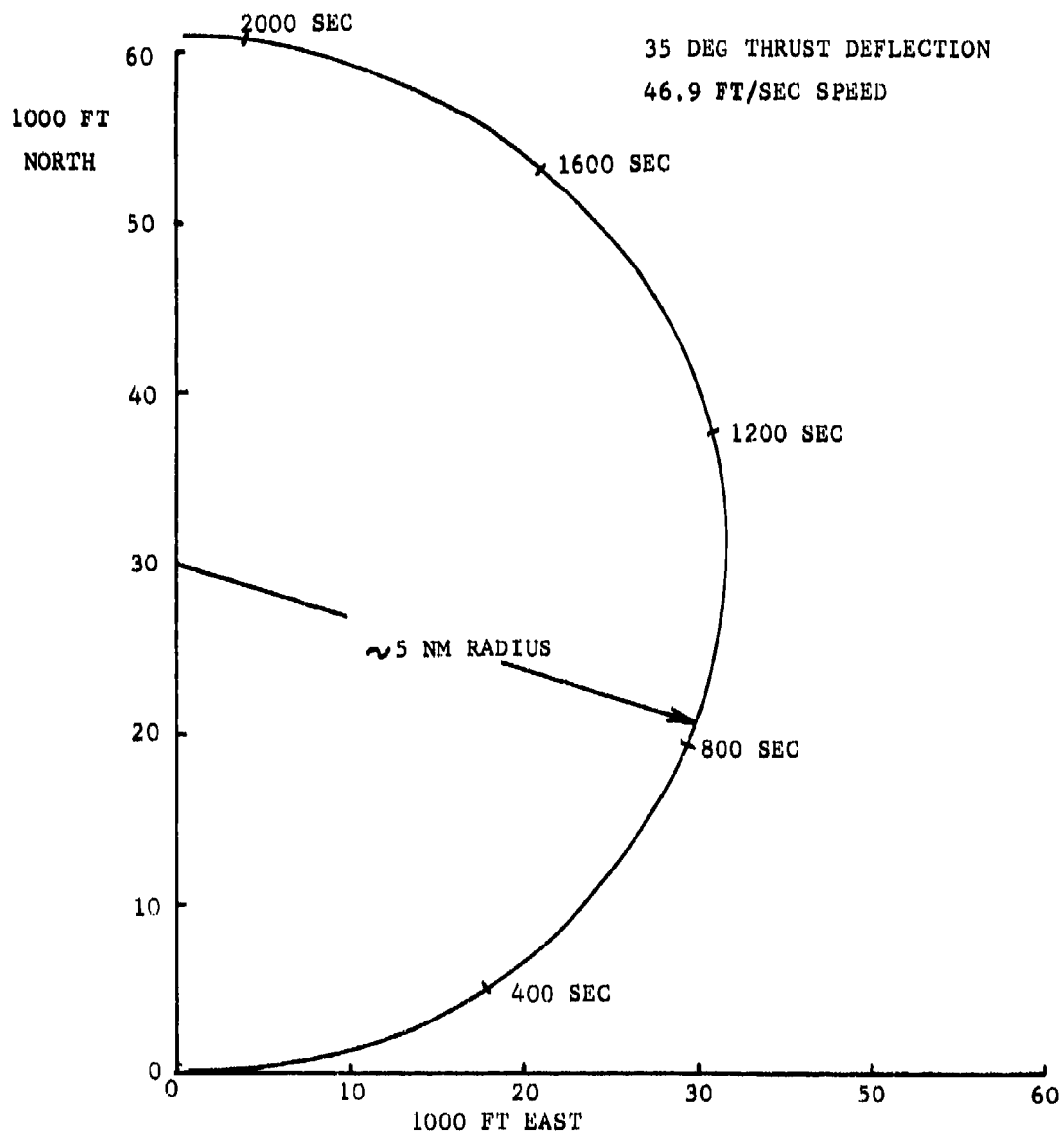
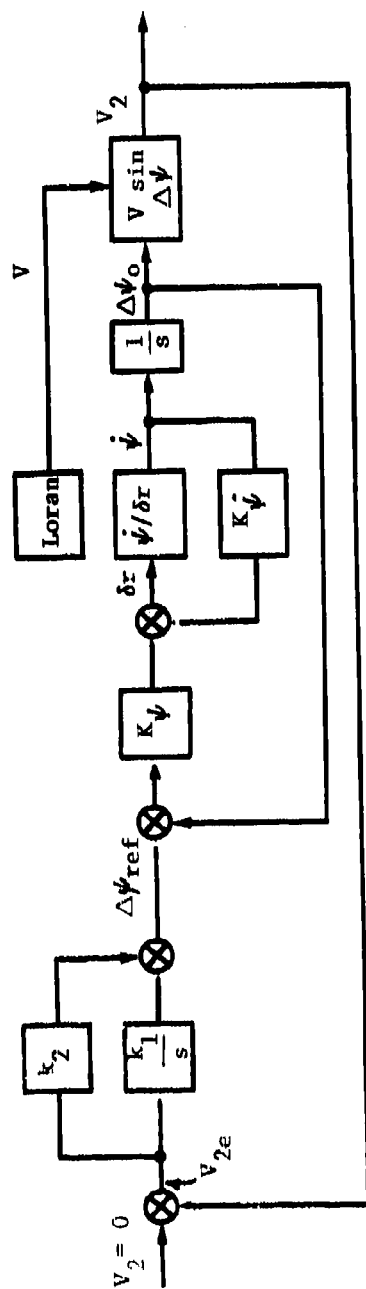


Figure A7: HI SPOT Airship Maximum Rate 180° Turn

navigation and heading control. This last approach is illustrated in Figure A-8, showing a Loran navigation signal coupled to the autopilot. As shown in the figure, the Loran system obtains the ground speed and direction, and compares this vector with the preset position coordinates to generate error signals to be acted on by the autopilot.



$$\dot{\psi} = -k_1 V_2 + k_2 \dot{V}_2$$

$$\int \dot{\psi} dt = \Delta\psi = -k_1 \int V_2 dt + k_2 V_2$$

$$\frac{V_2}{V} = \sin \Delta\psi, \text{ or } V_2 = V \sin \Delta\psi$$

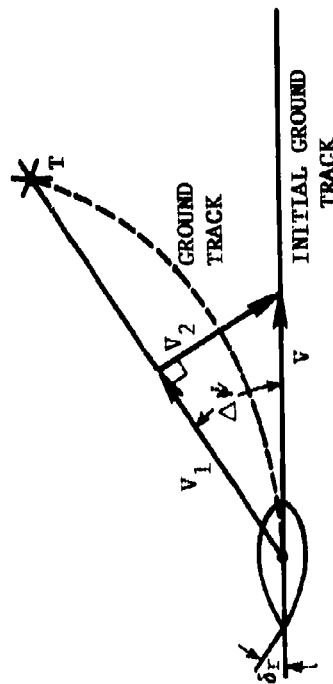


Figure A8: Steering Loop - Preliminary Concept

## APPENDIX "B"

### AEROSTAT SIZING

Aerostats are sized by specifying the initial altitude, cruise speed, dash speed, and powerplant type. Inherent in the program are a 200 lb, 800 watt payload; 200 watts additional auxiliary electrical power, and fuel for 30 days endurance; these can be changed by altering appropriate program statements. The program iterates to a solution by assuming an initial weight, computing the resultant envelope size, powerplant, and all component weights, then using the sum of the components as the next assumption until the assumed weight and the component sum differ by only a small amount. The component weights, aerostat dimensions, and selected performance characteristics are then printed.

The following symbols are used:

$C_D$  = aerostat drag coefficient,  $\text{Drag}/2 V_c^2 S_{\text{Ref}}$

$D$  = hull diameter, ft

$D_p$  = propeller diameter, ft

$h_1$  = initial altitude, ft

$h_2$  = final altitude, ft

$HP_c$  = cruise power required, horsepower

$HP_D$  = dash power required, horsepower

$L$  = hull length, ft

$N_p$  = propeller rotation speed, revolutions/min

$P_a$  = ambient air pressure,  $\text{lb}/\text{ft}^2$

$P_H$  = design hull pressure,  $\text{lb}/\text{ft}^2$

$Q_p$  = propeller torque at maximum power,  $\text{lb-ft}$

$S_{\text{Ref}}$  = aerostat reference area ( $V^{2/3}$ ),  $\text{ft}^2$

$S_T$  = total stabilizing fin area,  $\text{ft}^2$   
 $S_{\text{wet}}$  = hull wetted area,  $\text{ft}^2$   
 $\text{sfc}$  = specific fuel consumption,  $\text{lb/hr/HP}$   
 $U_C$  = average fuel consumption speed (cruise speed),  $\text{kt}$   
 $U_D$  = maximum dash speed,  $\text{kt}$   
 $V$  = hull volume,  $\text{ft}^3$   
 $W$  = total displacement weight,  $\text{lb}$   
 $W_D$  = speed reduction drive weight,  $\text{lb}$   
 $W_E$  = reciprocating engine weight,  $\text{lb}$   
 $W_F$  = gasoline fuel weight,  $\text{lb}$   
 $W_{FC}$  = regenerative fuel cell weight,  $\text{lb}$   
 $W_G$  = gondola weight,  $\text{lb}$   
 $W_H$  = hull weight (including fins),  $\text{lb}$   
 $W_{\text{He}}$  = displacement helium weight (99% purity),  $\text{lb}$   
 $W_L$  = payload weight,  $\text{lb}$   
 $W_{\text{LH}}$  = liquid hydrogen fuel weight,  $\text{lb}$   
 $W_M$  = electric motor weight,  $\text{lb}$   
 $W_P$  = propeller and hub weight,  $\text{lb}$   
 $W_Q$  = equipment and avionics weight,  $\text{lb}$   
 $W_R$  = contingency reserve weight,  $\text{lb}$   
 $W_{\text{RK}}$  = Rankine steam turbine system weight,  $\text{lb}$

$W_{SC}$  = solar cell array weight, lb

$W_T$  = fuel tank weight, lb

$\rho$  = ambient air density, slug/ft<sup>3</sup>

The ambient air pressure and density (assuming standard conditions) are closely approximated by the following functions:

$$P_a = 2625 / \exp(h_1 / 21032)$$

$$\rho = .004052 / \exp(h_1 / 20746)$$

The volume displaced by a given weight is

$$V = W / 32.17 \rho = 7.7615 W \exp(h / 20746)$$

From Figure 12, the geometric characteristics of the NACA 67030 profile as a body of revolution are:

$$L = 2.9564 V^{1/3}$$

$$D = .30L$$

$$S_{wet} = .6586 L^2$$

$$S_{Ref} = .11441 L^2$$

$$S_T = .07224 L^2$$

From a  $1/\sqrt{R_e}$  curve drawn through the data of Ref. 1, with 25% added for fin, gondola, and interference drag, the aerostat drag coefficient is:

$$C_D = .01926 / (\rho U_c L)^{1/2}$$

Assuming a day/night temperature ratio of 1.3, the maximum differential pressure sustained by the aerostat envelope is:

$$P_H = .30 P_a + 8.7526 W / L^2$$

The diameter of a propeller that converts 85% of its input power to thrust is:

$$D_p = .960 L / \sqrt{C_D}$$

The speed at which the propeller must rotate to achieve 85% efficiency is assumed to be an advance ratio of 0.9, and is:

$$N_P = 112.5 \ U/D_P$$

The torque required to turn the propeller at this speed is:

$$Q_P = W^{1/2} U_D^{5/2} / 22.24 N_P$$

The maximum power that must be produced by the aerostat powerplant is

$$HP_D = 1.457 + W^{1/2} U_D^{5/2} / 91346$$

The average cruise power that must be produced by the aerostat powerplant is:

$$HP_C = 1.457 + W^{1/2} U_C^{5/2} / 91346$$

From these equations, the following equations for the component weights are derived:

$$\text{Helium: } W_{He} = .14664 W$$

$$\text{Hull \& Fins: } W_H = L^3 P_H / 873291 + L^2 / 131.1$$

The first term represents Kevlar 49 yarn at a limit stress of 135,000 psi, while the second term represents aluminized mylar film and adhesive; fin weight is proportional to the fin area/hull area ratio; 10% is added for seams and reinforcements.

$$\text{Payload: } W_L = 200$$

$$\text{Reduction drive: } W_D = .050 Q_P$$

$$\text{Propeller \& hub: } W_P = .3196 D_P \left[ D_P (HP_D - 1.457) \right]^{1/3}$$

Powerplants and fuel:

$$\text{Reciprocating engine: } W_E = 27.6 HP_D^{.468}$$

$$\text{Specific fuel consumption: } sfc = .437 + .95 (.50 - HP_C / HP_D)^2$$

$$\text{Gasoline fuel: } W_F = W_1 \left[ \frac{360 \text{ sfc} \times HP_C}{W_1} \left( 2 - \frac{360 \text{ sfc} \times HP_C}{W_1} \right) \right]$$

$$\text{Rankine steam system: } W_{RK} = 10.2 HP_D$$

$$\text{Liquid hydrogen fuel: } W_{LH} = W_1 \left[ \frac{46.0 HP_C}{W_1} \left( 2 - \frac{46.0 HP_C}{W_1} \right) \right]$$

$$\begin{aligned}\text{Solar cell systems:} & \quad W_{SC} = 23.88 \text{ HP}_D \\ \text{Regenerative fuel cell:} & \quad W_{FC} = 54.96 \text{ HP}_C \\ \text{Electric motor:} & \quad W_M = 9.0(\text{HP}_D - 1.457)\end{aligned}$$

The regenerative fuel cell weight assumes 14 hr operation at average cruise power. 40 lb of onboard avionics, communications, antennas, instrumentation, and so forth, are assumed, plus 1/20 of the propulsion and drive system allowed for sensors and actuators:

$$W_Q = 40 + .05(W_D + W_L + W_E + W_{RK} + W_{FC} + W_M)$$

The fuel tank weight is assumed as 1/25 of the gasoline fuel or 1.135 times the cryogenic hydrogen fuel:

$$W_T = .04W_F + 1.135W_{LH}$$

The gondola weight includes 20 lb for impact attenuator, recovery system, and suspension, plus 1/25 of all equipment weight as enclosure and mounting systems, plus the fuel tanks:

$$W_G = 20 + W_T + .04(W_P + W_D + W_L + W_E + W_{RK} + W_{FC} + W_M + W_Q)$$

A contingency reserve of 10% of all hardware is set aside as an allowance for unexpected growth and unconservative assumptions in the weight equations:

$$W_R = .10(W - W_{He} - W_F - W_{LH})$$

Finally, the gross displacement must be the sum of all the component weights:

$$W = W_{He} + W_H + W_L + W_D + W_P + W_E + W_F + W_{RK} + W_{LH} + W_{SC} + W_{FC} + W_M + W_Q + W_T + W_G + W_R$$

If this sum does not equal the weight used to derive the envelope volume, helium weight, power required, etc., iteration must be performed.

Finally, as fuel is used, the fixed-volume envelope will ascend to higher altitude; the final equilibrium altitude will be:

$$h_2 = 20746 \ln \left[ \frac{V}{7.7615(W - W_F - W_{LH})} \right]$$

## APPENDIX "C"

### TECHNICAL CONTACTS

This appendix lists organizations and individuals that were consulted in assessing propulsion technology for the HI SPOT Program. In addition, Messrs. J. B. Hurley, T. E. Bailey, R. O. Hookway, S. H. Scales, and D. Lyles of the Martin Marietta Corporation, Denver Division, made valuable technical contributions to the study.

1. Airesearch Corporation, Los Angeles, CA  
H. Morgan  
R. Schultz
2. Naval Underwater Systems Center, Newport, RI  
R. Nadolink
3. B. H. Carmichael, Consultant, Capistrano Beach, CA
4. M. Taylor, Consultant, Seattle, WA
5. Kolbo Corp., Anaheim, CA  
L. Kolbo
6. NASA - Dryden Flight Research Center, Edwards, CA  
R. D. Reed
7. General Electric Co., Aircraft Systems, Div., Wilmington, MA  
J. Nutall
8. NASA - Johnson Space Center, Clear Lake City, TX  
J. Ackerman
9. Energy Technology, Inc., Cleveland, OH  
C. G. Martin  
T. Kolenz
10. Army Aviation Systems Command, Ft. Eustis, VA
11. Bell Helicopter Division, Textro Corp., Ft. Worth, TX  
J. E. Mangum
12. Princeton University, Dept. of Mechanical & Aerospace Sciences, Princeton, NJ  
Prof. H. C. Curtis
13. NASA - Lewis Research Center, Cleveland, OH  
D. Mikkelsen  
R. G. Ragdale
14. University of Denver, Denver, CO  
F. E. Lynch